Mapping-by-Sequencing Identifies *HvPHYTOCHROME C* as a Candidate Gene for the *early maturity 5* Locus Modulating the Circadian Clock and Photoperiodic Flowering in Barley

**Artem Pankin,*,1 Chiara Campoli,*,1 Xue Dong,* Benjamin Kilian,† Rajiv Sharma,† Axel Himmelbach,†
Reena Saini,‡ Seth J Davis,‡,§ Nils Stein,† Korbinian Schneeberger,* and Maria von Korff*,**,††,2**

*Max Planck Institute for Plant Breeding Research, D-50829 Cologne, Germany, †Leibniz Institute of Plant Genetics and Crop Plant Research, D-06466 Seeland (OT Gatersleben), Germany, §Department of Biology, University of York, YO10 5DD York, United Kingdom, ‡Department of Crystallography, A. Mickiewicz University, 60-780 Poznan, Poland, **Institute of Plant Genetics, Heinrich Heine University, 40225 Düsseldorf, Germany, and ††Cluster of Excellence on Plant Sciences "From Complex Traits Towards Synthetic Modules" 40225 Düsseldorf, Germany

ABSTRACT Phytochromes play an important role in light signaling and photoperiodic control of flowering time in plants. Here we propose that the red/far-red light photoreceptor *HvPHYTOCHROME C* (*HvPHYC*), carrying a mutation in a conserved region of the GAF domain, is a candidate underlying the *early maturity 5* locus in barley (*Hordeum vulgare* L.). We fine mapped the gene using a mapping-by-sequencing approach applied on the whole-exome capture data from bulked early flowering segregants derived from a backcross of the Bowman(*eam5*) introgression line. We demonstrate that *eam5* disrupts circadian expression of clock genes. Moreover, it interacts with the major photoperiod response gene *Ppd-H1* to accelerate flowering under noninductive short days. Our results suggest that HvPHYC participates in transmission of light signals to the circadian clock and thus modulates light-dependent processes such as photoperiodic regulation of flowering.

M ANY plants use seasonal cues, such as photoperiod or vernalization, to coincide the timing of reproductive development with optimal climate conditions. Cultivated barley (*Hordeum vulgare* L. subsp. *vulgare*), like most temperate cereal crops, is a long day (LD) plant with two growth types, winter and spring. Winter types accelerate flowering after a prolonged period of cold (vernalization), whereas spring barley does not respond to vernalization. The growth habit is determined by the interaction of two genes, *Vrn-H2*, a strong inhibitor of flowering under long day conditions and *Vrn-H1*

(also known as *HvVRN1*). *Vrn-H1* is upregulated during vernalization and represses *Vrn-H2* (Yan *et al.* 2003, 2004). A deletion of the *Vrn-H2* locus and deletions in a regulatory region of *Vrn-H1* cause a spring growth habit (Hemming *et al.* 2009; Rollins *et al.* 2013). In spring or vernalized winter barley, LDs strongly promote flowering, whereas short days (SDs) delay reproductive development. Flowering under LDs is controlled by the major photoperiod response gene *Ppd-H1* (Turner *et al.* 2005). *Ppd-H1* is a homolog of the *PSEUDO-RESPONSE REGULATOR* (*PRR*) genes implicated in the circadian clock of the model species *Arabidopsis thaliana* (L.) Heynh. (hereafter *Arabidopsis*). A natural mutation in the conserved CCT domain of *Ppd-H1* causes a reduced response to LDs and was selected in cultivation areas with long growing seasons (Turner *et al.* 2005; Von Korff *et al.* 2006, 2010; Jones *et al.* 2008; Wang *et al.* 2010). *Ppd-H1*, *Vrn-H1*, and *Vrn-H2* converge on the floral inducer *HvFT1* (*Vrn-H3*), a homolog of *Arabidopsis* florigen *FLOWERING LOCUS T* (*FT*). In barley, expression levels of *HvFT1* in the leaf correlate with flowering time. *Vrn-H2* represses *HvFT1* to counteract induction of *HvFT1* by

Ppd-H1 under LDs before vernalization (Hemming *et al.* 2008). After vernalization, *Ppd-H1* becomes dominant and controls *HvFT1* expression and flowering time under LDs (Turner *et al.* 2005; Campoli *et al.* 2012a).

In addition to the vernalization and photoperiod response genes, reproductive development is controlled by the *early maturity* (*eam*; also referred to as *earliness per se*) loci. The environmental effect on flowering phenotypes controlled by variation at these genes is reduced or completely removed. Two barley *eam* genes, *HvELF3* and *HvLUX1*, have recently been identified as homologs of the *Arabidopsis* circadian clock regulators *EARLY FLOWERING 3* (*ELF3*), and *LUX/ARRHYTHMO* (*LUX*), respectively (Faure *et al.* 2012; Zakhrabekova *et al.* 2012; Campoli *et al.* 2013). Mutations in these genes were linked to reduced photoperiod response and early flowering under both LD and noninductive SD conditions.

The circadian clock is an autonomous oscillator that produces endogenous biological rhythms with a period of ~24 hr. Conceptually, a circadian system can be divided into three parts: the central oscillator and input and output pathways. In *Arabidopsis*, the circadian system comprises at least three interlocking feedback loops. The core oscillator is composed of three negative feedback loops: (a) the inhibition of evening complex (EC) genes *ELF3*, *EARLY FLOWERING 4* (*ELF4*), and *LUX* by the rise of CIRCADIAN CLOCK ASSOCIATED 1 (CCA1) and LATE ELONGATED HYPOCOTYL (LHY) late at night; (b) the inhibition of *PRR* genes by the EC early at night; and (c) the inhibition of *LHY/CCA1* by TIMING OF CAB EXPRESSION 1 (TOC1) in the morning (Kolmos *et al.* 2009; Huang *et al.* 2012; Pokhilko *et al.* 2012). Furthermore, the evening-expressed GIGANTEA (GI) protein was proposed as a negative regulator of the EC, which in turn inhibits *TOC1* expression (Herrero *et al.* 2012; Pokhilko *et al.* 2012).

Light provides the circadian clock with diurnal entrainment signals. In plants, light is perceived and transduced by multiple photoreceptors including phytochromes, cryptochromes, and phototropins (Davis 2002). The phytochromes (PHY), which are apoproteins covalently bound to the chromophore, primarily detect and interpret the levels and ratio of red and far-red light in the environment. In darkness, phytochrome is synthesized as the physiologically inactive red-absorbing form, Pr. Upon illumination with red light, Pr is converted to the active far-red absorbing form, Pfr, which can be transformed back to Pr by far-red light. In the dark, Pfr-active phytochrome reverts to the inactive Pr form in a process referred to as "dark reversion" (Butler and Lane 1965). These interconvertible forms provide the plant with a cellular switch that can interpret information on spectral quantity and quality into a suitable response.

The diversity of phytochromes is organized in three major clades of *PHYA*, *PHYB*, and *PHYC*, with the former two present in all studied seed plant taxa (Mathews 2010). Plant phytochromes have been intensively studied, since they contribute to various developmental processes in plants such as flowering, shade avoidance, dormancy, germination, and stomatal development (Franklin and Quail 2010). Mutations in phytochrome genes affect flowering time in *Arabidopsis*, sorghum, and rice (Childs *et al.* 1997; Takano *et al.* 2005; Balasubramanian *et al.* 2006; Saidou *et al.* 2009; Osugi *et al.* 2011; Hu *et al.* 2013). However, very little is known about the diversity, function, and signaling pathways of barley phytochromes. Szücs *et al.* (2006) mapped the barley orthologs of *PHYA* (*HvPHYA*) and -*B* (*HvPHYB*) both to the short arm of chromosome 4H, and *PHYC* (*HvPHYC*) to the long arm of chromosome 5H at the same location as the vernalization gene *Vrn-H1*. According to Hanumappa *et al.* (1999), a chemically mutagenized barley genotype BMDR-1 contains a light-labile phyB. They demonstrated that it was responsible for the photoperiod insensitivity of this genotype and additionally implicated phyA in regulation of flowering via a distinct but interrelated pathway. A recent study in barley has suggested that variation at HvPHYC, an amino-acid substitution in the GAF domain, affected flowering time only under LDs and independently of the circadian clock (Nishida *et al.* 2013).

We identified the same candidate mutation in HvPHYC, which underlies the *early maturity 5* (*eam5*) locus, using whole-exome capture and a mapping-by-sequencing approach (Schneeberger *et al.* 2009; Mascher *et al.* 2013a) applied on a backcross population between the spring barley Bowman and the introgression line Bowman(*eam5*) (Druka *et al.* 2011). We add important information to the recent findings of Nishida *et al.* (2013) by demonstrating that *HvPHYC-eam5* genetically interacts with the major photoperiod response gene *Ppd-H1* to accelerate flowering under LDs and in particular under SDs. In contrast to findings by Nishida *et al.* (2013), expression analyses showed that HvPHYC-eam5 disrupts the circadian clock and acts in the same pathway as the evening complex genes *HvELF3* and *HvLUX1*. Diversity analysis indicated the presence of two major HvPHYC haplotypes separated by a synonymous (s) SNP and reduced nucleotide diversity at this locus. Interestingly, the HvPHYC-*eam5* allele was selected in barley cultivars from Japan despite the strong effect of this mutation on the barley clock. This invites further research into comparing physiological effects and the overall significance of the circadian clock on plant adaptation.

Materials and Methods

Plant material and growth conditions

Flowering time (days to awn emergence on the main spike) of the spring cultivar Bowman and three Bowman-derived introgression lines Bowman(*Ppd-H1*), Bowman(*eam5*), and Bowman(*Ppd-H1* + *eam5*) (kindly provided by R. Waugh, James Hutton Institute and by David Laurie, John Innes Centre) was recorded for 10–15 plants per genotype. To score flowering, plants were grown in soil in a glasshouse under SDs (10 hr light, 20°:14 hr dark, 18°) and LDs (16 hr light, 20°:8 hr dark, 18°). To investigate expression levels of *HvFT1*, replicate leaves were sampled 2 hr before light off

14 days and 28 days after sowing (DAS) under LDs and SDs, respectively. In addition, expression changes during development were analyzed in replicate samples of Bowman and Bowman(eam5) harvested once per week (2 hr before light off) for 3 weeks under LDs and 9 weeks under SDs. Diurnal and circadian expression of core clock and flowering time genes was tested under SDs (8 hr light, 20°:16 hr dark, 18°) and free-running conditions in Bowman and Bowman(eam5) grown in a controlled environment growth chamber (CEGC). After 14 days under SDs, leaf material was harvested every 2 hr for a total of 24 hr from the start of the light period (time point T0). Night samples (T10–T22) were collected in the dark. After SDs, plants were released into continuous light (light-light, LL) and constant temperature (20°) and sampled every 2 hr or 4 hr for 48 hr starting after 8 hr of continuous light (T8). Two biological replicates, comprising the second youngest leaves of three independent plants, were analyzed. In addition, expression of HvCCA1 was analyzed in the barley cultivars Azumamugi (F380S), Hayachinemugi (F380S), and its parental lines Kaikei 84 (F380S) and Yukiwarimugi (without F380S) under constant conditions after entrainment under SDs.

Meristem development was scored in Bowman and Bowman(eam5) grown in soil in a CEGC. The main stem of three plants per genotype was dissected starting 16 days after germination every 2–3 days under LDs and every 3–4 days under SDs until flowering. The experiment was stopped after 70 days under SDs when the shoot apical meristem (SAMs) of Bowman(eam5) had flowered, and those of Bowman did not further develop. Meristem development was scored following the Waddington scale (Waddington et al. 1983).

To investigate natural diversity of the candidate gene, a set of 110 wild and cultivated barley genotypes were selected from germplasm collections at the Max Planck Institute of Plant Breeding Research (MPIPZ) in Cologne (Badr et al. 2000), the Barley 1K collection (Hübner et al. 2009), the Barley Germplasm Center at Okayama University (http://www.shigen.nig.ac.jp/barley), and the University of Curkurova, Turkey (Hakan Özkan) (Supporting Information, Table S3).

Gene expression analysis

Gene expression was analyzed in leaf samples harvested from Bowman, Bowman(Ppd-H1), Bowman(eam5), and Bowman(Ppd-H1 + eam5) grown under LD and SD conditions, from a developmental series of leaf samples from Bowman and Bowman(eam5) and from diurnal and circadian sampling of Bowman and Bowman(eam5) leaves. In addition, expression of HvCCA1 was analyzed in circadian samples of the barley cultivars Azumamugi, Hayachinemugi, Kaikei 84, and Yukiwarimugi. Total RNA extraction, cDNA synthesis, and qRT-PCRs using gene-specific primers were performed as explained in Campoli et al. (2012a,b; 2013) and Habte et al. (2014). Additional primers are listed in Table S4.

Identification of a candidate gene using mapping by sequencing and segregation analysis

To determine the position of eam5 on genetic and physical maps, we found closest flanking RFLP markers with known nucleotide sequences using the GrainGenes CMap browser (BinMap 2005; http://wheat.pw.usda.gov/cgi-bin/cmap). Illumina's Barley Oligo Pool Array (BOPA) markers flanking the Bowman(eam5) introgression were as determined by Druka et al. (2011). The RFLP and BOPA markers were anchored to the Morex genomic contigs (IBSC 2012) using Blastn. Genetic and physical locations of the Morex contigs were extracted from Mascher et al. (2013a) and IBSC (2012), respectively. To refine the candidate region carrying the causative mutation, we used a mapping-by-sequencing approach applied on Bowman, Bowman(eam5), and a pool of 204 BC_1F_2 lines enriched for early-flowering genotypes. The BC_1F_2 lines flowering together or close to Bowman (eam5) were selected from 846 BC_1F_2 lines sown in March 2012 in the field at MPIPZ and scored for heading date together with the parental lines. Genomic DNA was extracted from leaves using the BioSprint 96 kit (Qiagen) according to the manufacturer's recommendations. DNA samples were quantified using Quant-iT PicoGreen assay (Invitrogen) with the Synergy 4 microplate reader (Biotek). DNA from 204 BC_1F_2 lines was pooled in equal amounts and along with Bowman, Bowman(eam5) enriched for a 61.6 megabase pair coding sequence target using in-solution whole-exome capture (Roche NimbleGen, Madison, WI; Mascher et al. 2013b).

Illumina sequencing of the enriched libraries generated 93 M, 80 M, and 211 M reads for the Bowman, Bowman (eam5), and the pool of BC_1F_2 lines, respectively. Reads were trimmed and aligned to the barley reference sequence (IBSC 2012) using BWA 0.59 with default parameters (Li and Durbin 2009). Only those reads that uniquely mapped to the reference sequence were retained. Samtools 0.1.19 was used to generate consensus pileup information (Li et al. 2009). SNPs distinguishing the two parental samples were extracted using VarScan 2.3.5 (Koboldt et al. 2009). SNPs supported by at least 30 reads with the nonreference allele frequency >95% in either Bowman or Bowman(eam5) were considered in downstream analyses. In the BC_1F_2 pool data, we estimated the frequencies of the Bowman(eam5) SNP alleles. Next, we estimated the median allele frequency for all SNPs within individual reference contigs that were anchored to the barley physical map (IBSC 2013) and calculated a locally weighted scatterplot smoothing (LOWESS) regression. We used SHOREmap 2.1 (http://www.shoremap.org) to calculate a mapping interval based on the median allele frequencies and the corresponding coefficients of variation (Schneeberger et al. 2009; Galvão et al. 2012).

Barley genes within the candidate mapping interval were extracted using the map published by Mascher et al. (2013a) and characterized by the gene ontology (GO) terms using Blast2GO 2.5 pipeline (Conesa et al. 2005). Genes related to

flowering and circadian clock were selected as candidate genes. To narrow the list of candidate genes down, we designed allele-specific codominant markers (sequence characterized amplified region, SCAR and cleaved amplified polymorphic sequence, CAPS) distinguishing candidate gene alleles from Bowman and Bowman(*eam5*) and analyzed their segregation with the flowering phenotype using $BC_1F_{2:3}$ lines. To extract allele-specific polymorphisms in the candidate genes, Bowman and Bowman(*eam5*) reads were assembled *de novo* into contigs using ABySS 1.3.7 assembler (single end, $k = 25$; Simpson *et al.* 2009). The contigs homologous to the candidate genes were identified using Blastn and aligned to extract SNPs to design allele-specific PCR markers. Allele-specific markers for the barley *VIP4*-like genes, which were absent from the exome-enrichment assay, were designed based on the Sanger sequencing data of PCR fragments (see primers in Table S4).

To create the $BC_1F_{2:3}$ population, one seed of each of the early BC_1F_2 plants was sown in the greenhouse under 10-hr short days. Flowering time was scored and leaf material was harvested for DNA extraction and genotyping. PCR reactions [1× Colorless GoTaq Buffer, 0.2 µM dNTPs, 0.5 µM primers, 1 unit GoTaq polymerase (Promega, Mannheim, Germany), 50 ng DNA] were incubated in the PTC-200 DNA Engine thermocycler (Bio-Rad, Hercules, CA) and visualized using agarose gel electrophoresis. The primer sequences and incubation regimes were as in Table S4. Restriction of the CAPS PCR fragments was performed using endonucleases (New England Biolabs, Frankfurt am Main, Germany) following the manufacturer's recommendations.

Natural diversity and population-genetic analyses

Barley genomic DNA was extracted using the DNAeasy 96 Plant kit (Qiagen, Hilden, Germany) according to the manufacturer's recommendations and quantified using NanoDrop 1000 spectrophotometer (Thermo Scientific, Wilmington, DE). A 2045-bp fragment covering exon 1 of *HvPHYC* was amplified from a set of 113 wild and cultivated barley genotypes using the primer pairs Ex1seq_1f + Ex1seq_1r and Ex1seq_2f + Ex1seq_2r (Table S4). PCR reactions [1× Q5 buffer, 0.2 µM dNTPs, 0.5 µM primers, 1 unit Q5 High-Fidelity DNA Polymerase (New England Biolabs), 50 ng DNA] were incubated in a PTC-200 DNA Engine thermocycler (Bio-Rad). PCR fragments were purified using 1.8× Agencourt AMPure XP beads (Beckman Coulter, Krefeld, Germany) following the manufacturer's recommendations and Sanger sequenced. Three additional *HvPHYC* sequences were extracted from National Center for Biotechnology Information (NCBI) GenBank (DQ201145, DQ201146, and DQ238106). Haplotype analysis was performed as described in Campoli *et al.* (2013). Nucleotide diversity π was calculated for the coding region using DnaSAM v. 20100621 (Eckert *et al.* 2010).

Motif conservation analysis and protein modeling

Positions of the GAF and PAS domains at HvPHYC were determined using InterProScan (Quevillon *et al.* 2005). A set of 4419 protein sequences of the PHY homologs from plant and bacterial species were extracted using Blastp search in the NCBI "nr" database with a 70-bp conserved fragment of the HvPHY GAF domain as a query (cut-off *e*-value 1*e*-7). The PHY homologs were aligned using MAFFT v6.851b ("auto" model selection) and PRANK v.130820 (default parameters, +F) (Loytynoja and Goldman 2005; Katoh and Toh 2008). Amino-acid polymorphisms at HvPHYC were discovered by translating exon 1 fragments comprising nonsynonymous (ns) SNPs using ExPASy Translate tool (http://web.expasy. org/translate). The 8- to 15-aa subalignments around these polymorphic sites were submitted to the WebLogo generator (Crooks *et al.* 2004). Visually misaligned regions flanking the polymorphic amino-acid residues outside the GAF domain were iteratively realigned in a smaller subset of the PHY sequences. In addition, the functional effect of the amino-acid substitutions was predicted using PROVEAN (cut-off score −2.5) (Choi *et al.* 2012).

Structural modeling was carried out with the I-TASSER approach (Zhang 2008). Models were generated for the chromophore-bearing region of HvPHYC for both the Bowman and Bowman(*eam5*) alleles. Structural alignment of the models was performed with the University of California San Francisco Chimera package (Pettersen *et al.* 2004).

Statistical analysis

Significant differences in flowering time, meristem development, and gene expression between Bowman, Bowman(*eam5*), and Bowman(*eam5 + Ppd-H1*) were calculated using a paired *t*-test ($P < 0.05$). For diurnal and circadian gene expression, statistical significance was calculated using a general linear model in the SAS software 9.1.3 (SAS Institute 2009) with the factors genotype, time point, biological replicate, and first-order interaction effects. Significant differences ($P < 0.05$) between least-squares means of the genotype-by-time interactions were calculated using a Tukey–Kramer adjustment for multiple comparisons.

Results

Bowman(eam5) is early flowering under SD and LD conditions

We analyzed the effects of *eam5* on photoperiod-dependent flowering in barley and its genetic interaction with the major barley photoperiod response gene *Ppd-H1*. Bowman, Bowman(*eam5*), Bowman(*Ppd-H1*), and Bowman(*Ppd-H1 + eam5*) plants were scored for flowering time under LD and SD conditions in controlled greenhouse settings (Figure 1A). Under LDs, Bowman(*Ppd-H1*) and Bowman(*Ppd-H1 + eam5*) flowered first, both at 28 DAS. Bowman(*eam5*) flowered at 42 DAS, followed by Bowman at 45 DAS. Under SDs, Bowman(*Ppd-H1 + eam5*) flowered 57 DAS, followed by Bowman(*eam5*) with 65 DAS, while Bowman and Bowman(*Ppd-H1*) flowered on average 88 and 91 DAS, respectively. Thus *eam5* accelerated flowering time under both LD and SD conditions.
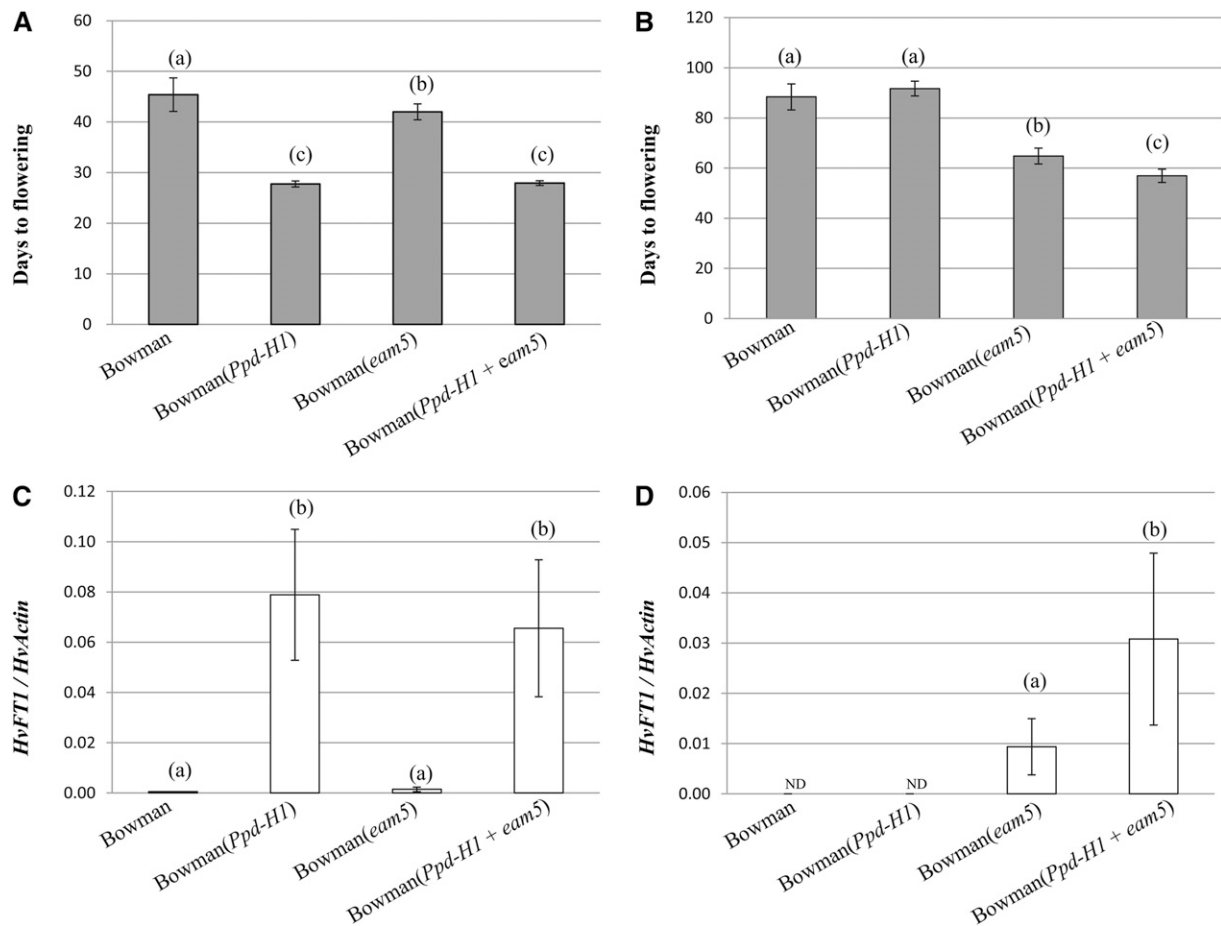
Figure 1 Flowering time and *HvFT1* expression levels of Bowman and introgression lines. Bowman and Bowman introgression lines carrying different combinations of *Ppd-H1* and *eam5* alleles were grown under long days (16-hr light/8-hr darkness; LD, A and C) or short days (10-hr light/14-hr darkness, B and D). (A and B) Flowering time is shown as mean days to awn emergence on the main stem. Error bars are standard deviations for 8–15 plants of each genotype. (C and D) *HvFT1* expression relative to *HvActin* is shown as average of three biological and two technical replicates plus/minus standard deviation. Leaf material was sampled after 2 weeks (LD) and 5 weeks (SD) 2 hr before light off. Genotypes with different letters are significantly different ($*P < 0.05$). NF, not flowering; ND, not detectable.

It is notable that, under SDs, *Ppd-H1* accelerated flowering time in the background of *eam5*.

We determined the effect of *eam5* on the development of the SAM by scoring its morphological changes in Bowman and Bowman(*eam5*) plants starting 2 weeks after germination until heading (Figure S1). Under both LD and SD conditions, the SAM of Bowman(*eam5*) developed significantly faster than that of Bowman. Under SDs, differences in SAM development between the genotypes became manifest only after Waddington stage 4: the SAM of Bowman(*eam5*) developed until flowering, while the SAM of Bowman remained at this stage until 70 DAS. Under LDs, the SAM started to develop significantly faster in Bowman(*eam5*) than in Bowman after Waddington stage 3. These differences in SAM development suggested that *eam5* primarily affects inflorescence development and stem elongation.

To test whether differences in the expression of *HvFT1* correlated with the observed flowering-time phenotypes, we measured its expression in the different Bowman introgression lines under LDs and SDs, respectively (Figure 1, C and D).

After 2 weeks under LDs, *HvFT1* showed a low but detectable expression in Bowman and Bowman(*eam5*), which was significantly lower than *HvFT1* expression in Bowman (*Ppd-H1*) and Bowman(*Ppd-H1* + *eam5*). After 4 weeks under SDs, *HvFT1* expression was detected only in Bowman(*Ppd-H1* + *eam5*) and Bowman(*eam5*). Therefore, we suggest that the *eam5* mutation accelerated flowering time under both LDs and SDs through an upregulation of *HvFT1*.

Identification of barley PHYC as a candidate gene underlying *eam5*

The *eam5* locus was described as a mutation of unknown origin isolated from an ICARDA/CIMMYT selection CMB85-533 (Higuerilla*2/Gobernadora) and mapped onto chromosome 5H (Jain 1961; Franckowiak 2002). Like many other barley QTL, *eam5* has been introgressed into the spring barley cultivar Bowman (Druka *et al.* 2011). The resultant BC$_6$ introgression line Bowman(*eam5*) (also referred to as BW285) was genotyped using the SNP-based array (Illumina's BOPA) with 3072 SNPs (Close *et al.* 2009). This revealed a single
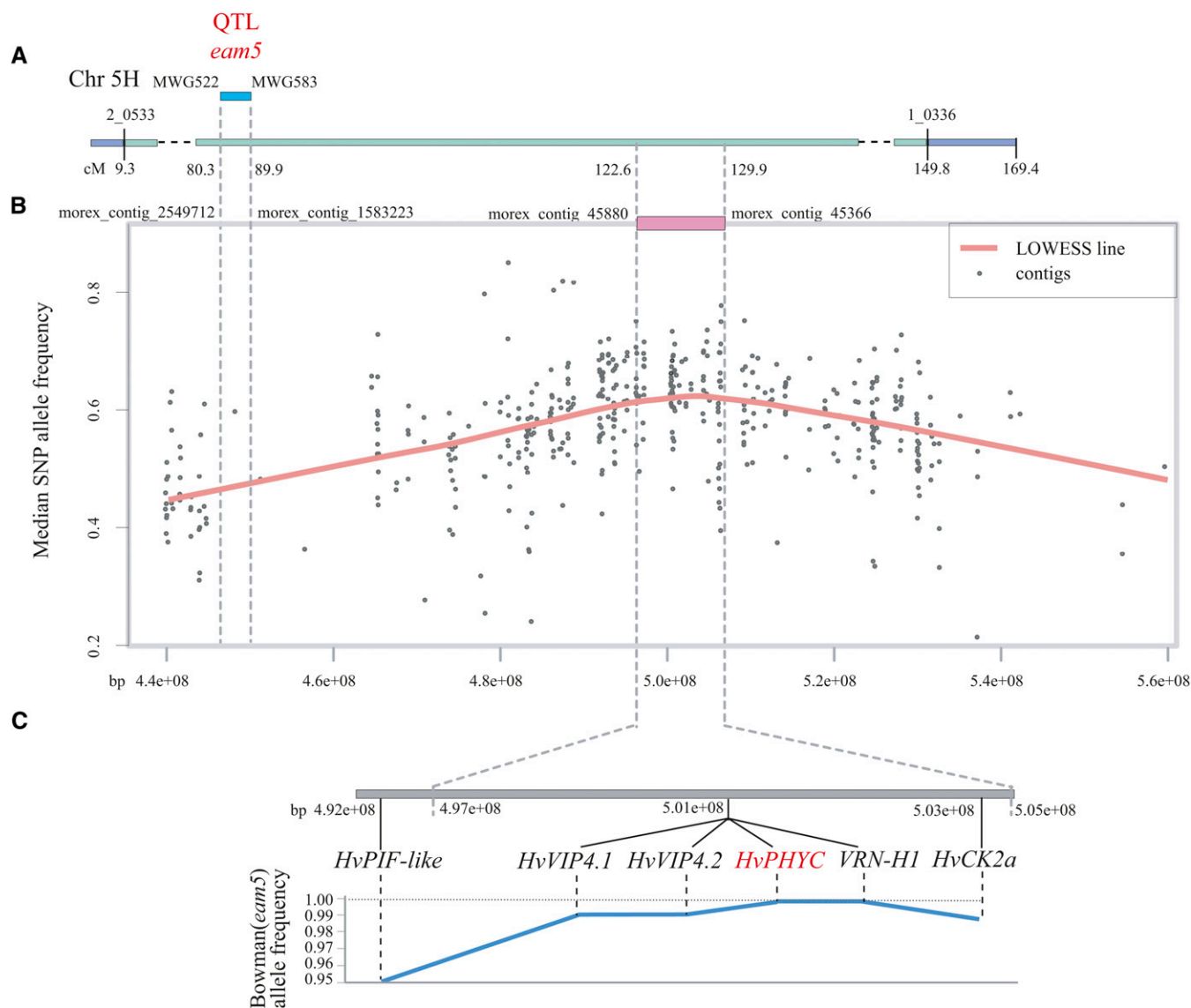
Figure 2 Identification of *HvPHYC* as a candidate gene for the *eam5* QTL. Corresponding regions of the genetic and physical maps are connected with gray dashed lines. (A) Location of the *eam5* QTL on the Bowman(*eam5*) introgression. A 144-cM introgression on chromosome 5 of the Bowman(*eam5*) line and Bowman background are shown, respectively, as green and blue bars. The BOPA markers flanking the introgression and the corresponding genetic distances (in centimorgans) are above and below the bars, respectively. The tentative location of the *eam5* QTL is shown as a blue rectangle with genetic markers flanking the QTL. (B) QTL position refinement using bulk segregant high-throughput sequencing and SHOREmap (Schneeberger *et al.* 2009). Median SNP allele frequencies are plotted along the physical map of barley chromosome 5H in the vicinity of the *eam5* QTL. The QTL interval as calculated by SHOREmap is shown as a magenta bar together with the flanking contigs. Numbers on the *x*-axis are distances on the barley physical map (IBSC 2012) in pairs of nucleotides. LOWESS, locally weighted scatterplot smoothing. (C) Segregation analysis of the candidate genes within the SHOREmap QTL region. Six flowering-related candidate genes are located in or near the SHOREmap QTL region (gray bar). Frequencies of the Bowman(*eam5*) alleles in BC$_1$F$_{2:3}$ plants that flowered, excluding heterozygous genotypes, are plotted along the barley physical map (IBSC 2012). The highest allele frequency indicates the best candidate genes for the *eam5* QTL.

introgression on chromosome 5H of Bowman(*eam5*) flanked by the BOPA markers 2_0533 (9.3 cM as morex_contig_64122) and 1_0336 (149.8 cM as morex_contig_2550061). *eam5* was mapped between RFLP markers MWG522 (80.3 cM as morex_contig_2549712) and MWG583 (89.9 cM as morex_contig_1583223) (Figure 2A). To delineate the candidate gene underlying the *eam5* mutation, we backcrossed the introgression line Bowman(*eam5*) with Bowman and scored heading date in the field. Of the 846 phenotyped BC$_1$F$_2$ lines, 204

genotypes were selected as flowering at the same time as Bowman(*eam5*), which flowered on average 4 days earlier than Bowman and the remaining population.

To refine the *eam5* interval, we used a mapping-by-sequencing approach applied on the parental lines Bowman and Bowman(*eam5*) and the pool of BC$_1$F$_2$ lines enriched for early flowering genotypes. We reduced the complexity of the barley genome using whole-exome capture (Mascher *et al.* 2013b), which targeted sequencing on the gene space. On

average, 92% of the Illumina reads aligned against the targeted regions and were used to discover SNPs between the samples and the reference sequence. We identified 3884 SNPs that were specific for either Bowman or Bowman(eam5). Of those, 2929 SNPs resided in 640 contigs located on the barley physical map (IBSC 2012). To estimate Bowman (eam5) allele frequency at each of these marker sites within the pool of BC_1F_2, we used SHOREmap (Schneeberger et al. 2009). Using the median-allele frequency of SNPs within each contig and their physical location, it identified a probabilistic QTL mapping interval of 8 Mb located on the chromosome arm 5HL and comprising 210 genes according to the most current POPSEQ barley map (Figure 2B; Mascher et al. 2013a). The maximum SNP allele frequencies of Bowman(eam5) approached 75% due to the presence of heterozygous genotypes in the pool of BC_1F_2 lines selected from the field experiment. The presence of heterozygotes in the pools was verified by phenotyping and genotyping in $BC_1F_{2:3}$ lines derived from the pooled plants as explained below.

The GO analysis identified five candidate genes related to flowering time or circadian clock within this 8-Mb interval. Four of them, *HvPHYC* (MLOC_824), *VRN-H1* (AK360697), *HvVIP4.1* (MLOC_17672), and *HvVIP4.2* (MLOC_17943), which are, respectively, homologs of *Arabidopsis* genes *PHYC* (AT5G35840), *APETALA 1* (AT1G69120), and *VERNALIZATION INDEPENDENCE 4* (AT5G61150), mapped to the same location on the chromosome arm 5HL. The fifth gene *HvCK2α* (MLOC_55943), a homolog of *Arabidopsis CASEIN KINASE 2 ALPHA* (AT2G23070), resided 2 Mb downstream of this cluster of four genes. Another flowering-related gene *HvPIF*-like (AK362162), a homolog of *Arabidopsis PHYTOCHROME-INTERACTING FACTOR* genes, located 9 Mb upstream of the unresolved cluster of the four candidate genes was also selected for the fine mapping.

Segregation analysis of the candidate genes was conducted in $BC_1F_{2:3}$ lines, derived from the early flowering BC_1F_2 plants. Analysis of flowering time in 180 $BC_1F_{2:3}$ under SD conditions in the glasshouse revealed that the phenotype followed a trimodal distribution. A total of 108 lines were scored as early, which flowered within 10 days after Bowman (eam5), whereas 17 lines flowered significantly later frequently showing abnormalities in the spike development. The rest of the 55 lines did not flower until the end of the experiment. Therefore, we suggested that *eam5* was a semidominant locus with the heterozygote exhibiting an intermediate phenotype.

We reconstructed Bowman and Bowman(eam5) alleles of the candidate genes from the *de novo* assembly of the exome reads. Allele-specific polymorphisms were tagged with codominant SCAR and CAPS markers used for screening of the $BC_1F_{2:3}$ lines. The segregation analysis revealed that both *Vrn-H1* and *HvPHYC* were tightly linked to the early flowering phenotype; all plants carrying Bowman(eam5) alleles at these genes flowered, plants with Bowman alleles did not flower until the end of the experiment, and heterozygotes exhibited an intermediate phenotype. No recombinants were detected between *Vrn-H1* and *HvPHYC* (Figure 2C). *Vrn-H1* and *HvPHYC* reside only five

gene models apart based on the better resolved *Brachypodium* map. Using allele-specific markers reported by Hemming et al. (2009), we discovered that Bowman carries the *HvVRN1-1* spring allele with a 5154-bp deletion in the first intron, whereas Bowman(eam5) contains the *HvVRN1* winter allele without an intron deletion. This winter allele is known to strongly delay flowering in the absence of vernalization (Hemming et al. 2009).

HvPHYC carried a nonsynonymous mutation (T/C) in Bowman(eam5). This caused the missense substitution that leads to a change of the hydrophobic phenylalanine to the hydrophilic serine (mutation F380S) within a previously uncharacterized extremely conserved motif in the GAF domain of phytochromes (Figure 3). At this position, phenylalanine is exclusively present in 4267 phytochrome homologs from 2799 species of Plantae and Bacteria kingdoms present in GenBank. The conservation analysis using the PROVEAN tool predicted that the F380S mutation could be functional (observed score −7.673; cut-off score −2.5). Taken together, our analyses strongly suggested that the F380S substitution could be critical for the HvPHYC function and thus we propose *HvPHYC* as the candidate gene underlying *eam5*.

Diversity analysis of HvPHYC and its linkage with VRN-H1 alleles

To explore natural diversity of barley *HvPHYC* alleles, we sequenced a 2045-bp fragment of the first exon comprising conserved domains from 52 wild (*H. vulgare* L. subsp. *spontaneum* (K. Koch) Thell.), 56 cultivar and landrace, and 3 *H. agriocrithon* A. E. Åberg genotypes. In addition, three *HvPHYC* sequences from cultivars were extracted from the NCBI GenBank. We identified 15 haplotypes, of which 6 haplotypes were specific for cultivated accessions, 6 haplotypes for wild, and 3 haplotypes were common to both groups (Figure 4; Table S1). The nucleotide diversity of *HvPHYC* haplotypes, which were defined by 13 ns and 8 s SNPs within the coding region, was low ($\pi = 0.46 \times 10^{-3}$). Haplotypes 1 and 2 were most frequent; 84 of 114 genotypes carried these two haplotypes.

We attempted to predict a functional effect of the observed nonsynonymous SNPs based on the protein conservation patterns. The motif conservation analysis revealed two extremely conserved amino-acid substitutions, which were additionally identified by PROVEAN as deleterious (Table S2). One of the mutations, F380S, which was found in Bowman(eam5), also appeared in 10 Japanese cultivars (haplotype 4; Table S3), whereas another mutation, L364D was found in addition to F380S in Japanese cultivar Azumamugi (haplotype 7).

Based on the result of the segregation analysis, we assumed that the Bowman(eam5) *HvPHYC* allele and wild-type *HvVRN1* are tightly linked. To verify this fact, we screened 10 other "haplotype 4" genotypes with markers specific for the wild-type *HvVNR1* allele. Without exception, the Bowman(eam5) *HvPHYC* allele was linked to the winter type *HvVRN1* allele (Table S3).
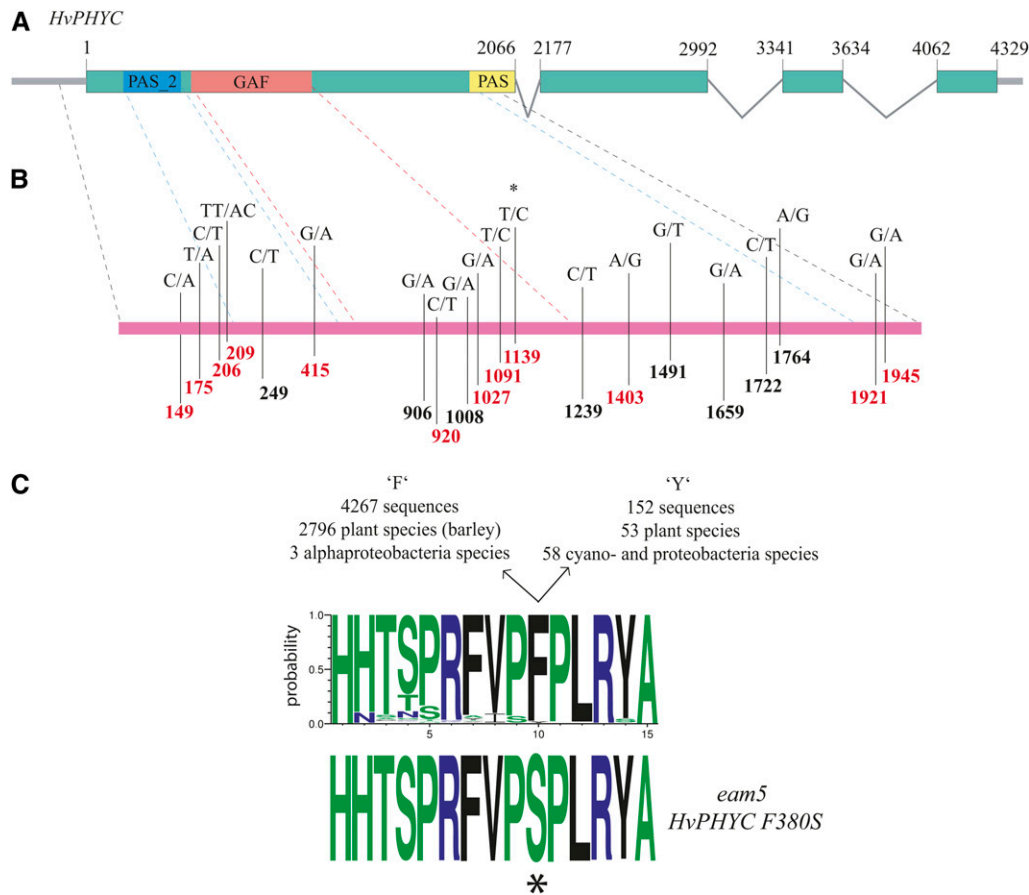
Figure 3 The structure of the barley (*Hordeum vulgare*) *HvPHYC* gene, polymorphisms in the exon 1 and effect of the *eam5* mutation. (A) The diagrammatic structure of the *HvPHYC* gene and location of the conserved domains on exon 1. The exons and introns are respectively shown by green rectangles and lines angled downward. The coordinates are shown in pairs of nucleotides relative to the first coding nucleotide of the full-length "Morex" *HvPHYC* sequence (DQ238106). The conserved domains PAS_2 (IPR013654), PAS (IPR000014), and GAF (IPR03018) are highlighted in blue, yellow, and red, respectively. (B) Nucleotide variation in a 2045-bp fragment of *HvPHYC* exon 1. The resequenced fragment comprising exon 1 of *HvPHYC* is shown as a magenta bar. SNPs are shown above the bar (major/minor alleles) and the coordinates, which are also unique SNP identifications, below the bar. Nonsynonymous SNPs are highlighted in red font. Correspondence of the polymorphic sites to the conserved domains is depicted by dashed lines. (C) Conservation of the motif in the GAF domain of the phytochrome gene family and the effect of the *eam5* mutation. An alignment of 4419 sequences of the extremely conserved motif in the GAF domain from the plant and bacteria *PHY* genes is shown as a sequence logo. Green letters, neutral amino-acid residues (aa); black, hydrophobic aa; blue, hydrophilic aa. The aa substitution in the *eam5* line is shown by an asterisk.

eam5 affects the expression of circadian clock genes

Previous studies have shown that the circadian clock mediates light signaling to downstream components of the photoperiod-response pathway in *Arabidopsis* and barley (Onai and Ishiura 2005; Faure *et al.* 2012; Campoli *et al.* 2013). To investigate whether the *eam5* mutation affected the barley circadian clock, we studied diurnal (under SDs) and circadian LL expression of barley clock homologs, *HvCCA1*, *Ppd-H1* (*HvPRR37*), *HvPRR73*, *HvPRR59*, *HvPRR95*, *HvPRR1*, *HvGI*, *HvELF3*, *HvELF4*, and *HvLUX1* in Bowman and Bowman(*eam5*) (Figure 5A, Figure S2).

Under SDs, Bowman(*eam5*) showed significantly reduced expression of *HvPRR73*, *HvELF3*, *HvELF4*, and *HvPHYC* compared to Bowman at the peak time of expression. The SD expression of all other tested clock genes was not significantly different between genotypes. Under LL conditions, the expression patterns of *HvCCA1*, *Ppd-H1* (*HvPRR37*), *HvPRR73*, *HvGI*, and *HvPRR1* were significantly different between Bowman and Bowman(*eam5*). Under these conditions, in Bowman(*eam5*), circadian amplitude of *HvCCA1* expression was strongly reduced during the subjective days, while *Ppd-H1* was significantly upregulated in Bowman(*eam5*) compared to Bowman at most time points. In contrast to *Ppd-H1*, expression

of its homolog *HvPRR73* was significantly lower in Bowman(*eam5*) than in Bowman during the subjective day. Expression of the evening expressed genes *HvGI* and *HvPRR1* was significantly higher in Bowman(*eam5*) than in Bowman during subjective nights. Finally, *HvPHYC* expression was significantly lower in Bowman(*eam5*) during the subjective day. Circadian expression of *HvLUX1*, *HvPRR59*, *HvPRR95*, *HvELF3*, and *HvELF4* was not strongly affected by the *eam5* mutation. In Bowman(*eam5*), peak expression of *HvCCR2*, encoding the barley ortholog of the *GYLCINE-RICH RNA-BINDING PROTEIN 7* (*GRP7/CCR2*), characterized as a slave (nonself-sustaining) oscillator (Schöning and Staiger 2005), was reduced under SD and LL compared to Bowman (Figure 5B). Taken together, these results indicate that *eam5* alters the expression of barley homologs of *Arabidopsis* clock genes, in particular the expression of *HvCCA1* and *Ppd-H1*.

In *Arabidopsis*, expression of genes implicated in regulation of photoperiod-dependent flowering is under circadian control. We therefore tested whether *eam5* changed the diurnal and circadian expression of the photoperiod response genes *HvCO1*, *HvFT1*, and *Vrn-H1* (Figure 5B). Under SDs, *HvCO1* was significantly higher expressed in Bowman(*eam5*) than in Bowman in SDs and LL (Figure 5B). *HvFT1*
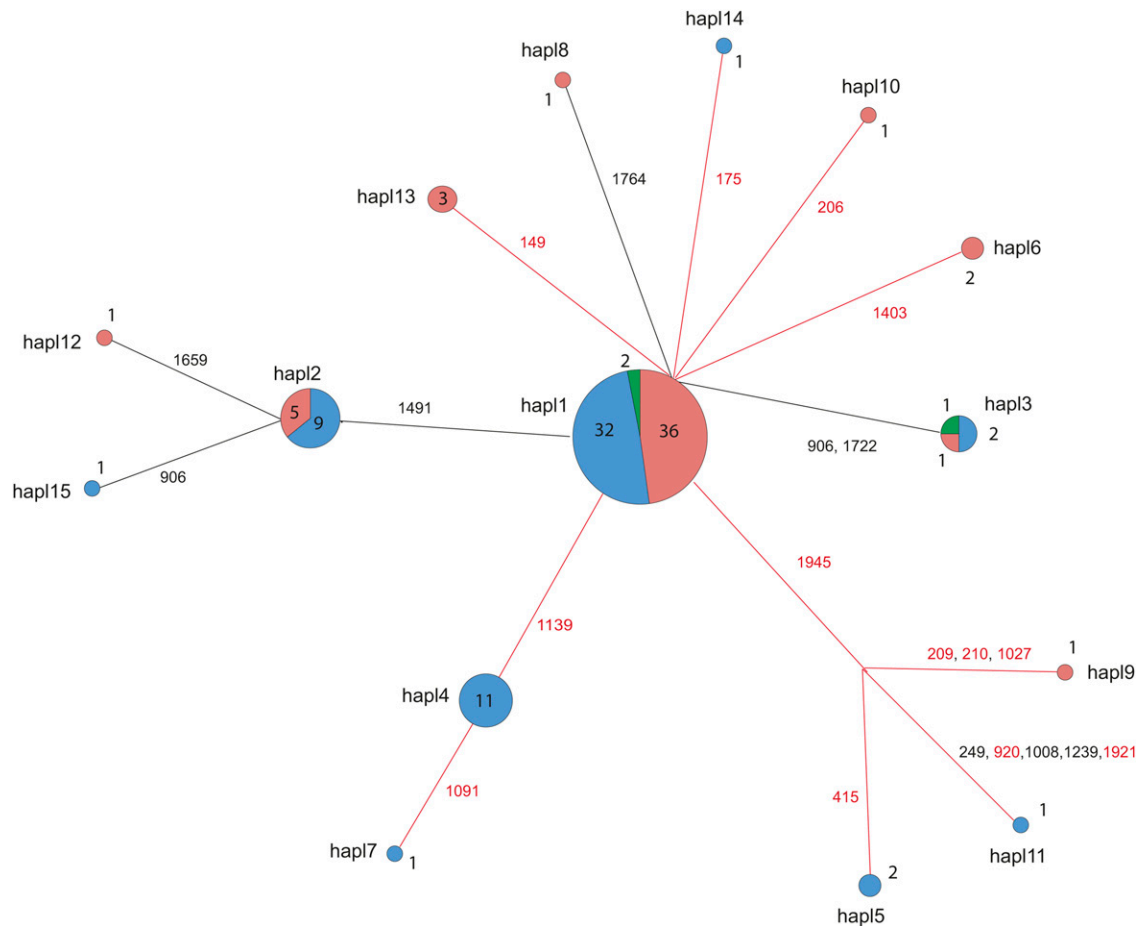
Figure 4 Median-joining network of 15 *HvPHYC* haplotypes. Numbers at the nodes indicate the number of genotypes carrying the corresponding haplotype (of 114 accessions). The haplotype frequency is also reflected in the relative size of a node. The color of a node corresponds to the different species: blue, *Hordeum vulgare* subsp. v*ulgare*; red, *H. vulgare* subsp. *spontaneum*; green, *H. agriocrithon*. Numbers at the branches denote synonymous (in black) and nonsynonymous (in red) SNPs (as on Figure 3) separating the haplotypes.

expression was not detected under SDs in any of the two genotypes at 14 DAS, whereas Bowman(*eam5*) exhibited a strong upregulation of *HvFT1* during the subjective day in LL compared to Bowman. The spring *Vrn-H1* allele was expressed and showed circadian oscillations in Bowman, but the winter *HvVRN1* allele in Bowman(*eam5*) was not expressed at 14 DAS under SDs (Figure 5B). This corroborates our suggestion that *HvVRN1* was not involved in the early flowering of Bowman(*eam5*). In addition, we have previously shown that variation between the winter and spring *HvVRN1* alleles did not affect the circadian clock (Faure *et al.* 2012). Taken together, flowering time data and the expression analysis excluded *HvVRN1* as a gene underlying *eam5*.

To corroborate the link between *eam5/HvPHYC* and the circadian clock, we examined different lines carrying the *HvPHYC* F380S allele (haplotypes 4 and 7) for variation in the circadian expression of the marker gene *HvCCA1* (Figure S3). The expression of *HvCCA1* in Hayachinemugi and Kaikei 84 (both with F380S, haplotype 4) was markedly dampened during the subjective day compared to Yukiwarimugi (without F380S). Therefore, the effect of F380S in Japanese

lines was similar to the *HvCCA1* expression differences between Bowman and Bowman(*eam5*). Expression of *HvCCA1* in Azumamugi (with F380S and L364D, haplotype 7) was also significantly lower than in Yukiwarimugi, but higher than in Kaikei 84 and Hayachinemugi. Based on these data, we conclude that the F380S mutation in HvPHYC correlated with variation in circadian expression of *HvCCA1* also in Japanese cultivars. However, quantitative variation in *HvCCA1* expression between different HvPHYC F380S lines suggested the presence of modifying genes.

Discussion

HvPHYC is a candidate gene underlying eam5

In this study, we describe the barley locus *eam5*, which accelerated flowering under LDs and in addition, led to flowering under noninductive SDs. To fine map the *eam5* mutation, we used mapping-by-sequencing of bulked early flowering BC_1F_2 lines, followed by candidate-gene mapping in $BC_1F_{2:3}$. Fine mapping-by-deep sequencing has been successfully applied in model species to map and identify
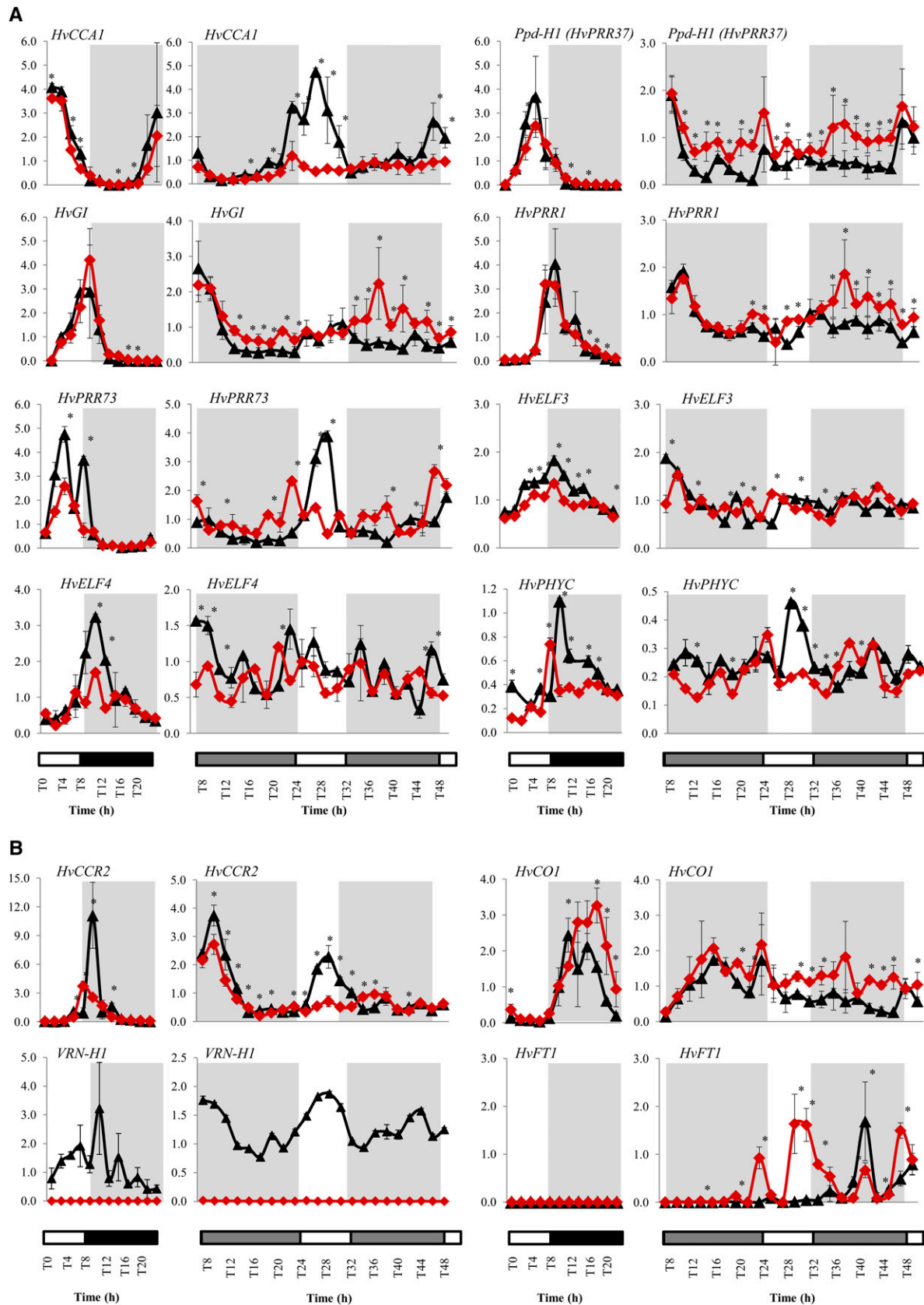
Figure 5 Expression patterns of circadian clock and clock output genes. Expression of (A) circadian clock genes *HvCCA1*, *Ppd-H1* (*HvPRR37*), *HvGI*, *HvPRR1*, *HvPRR73*, *HvELF3*, *HvELF4*, and *HvPHYC* and (B) the clock output gene *HvCCR2* and the flowering genes *HvCO1*, *HvVRN1*, and *HvFT1* in Bowman (black lines) and Bowman(*eam5*) plants (red lines) under SD and constant conditions. White, black, and gray bars indicate days, nights, and

induced mutations underlying a specific phenotype in a single step (James *et al.* 2013). We demonstrate that this method is also effective in fine mapping a mutation in the large genome of a crop plant. We found that the use of an introgression line with prior mapping information and exome enrichment greatly reduced the complexity of the task (Druka *et al.* 2011; IBSC 2012; Mascher *et al.* 2013b). Mascher *et al.* (2013b) have demonstrated that fine mapping of barley genes has become feasible due to the recent release of the barley gene space reference sequence and advances in the physical and genetic mapping (IBSC 2012; Mascher *et al.* 2013a). As a proof of concept, using a simulated *in silico* bulk-segregant analysis, they showed that a qualitative row-type gene *Vrs1* could be fine mapped to a relatively small interval containing 128 genes (Mascher *et al.* 2013b). We demonstrate that fine mapping through exome capture and deep sequencing of a BC_1F_2 pool was successful, even though the phenotype was quantitative, subtle, and obscured by the segregation of another tightly linked flowering gene. The identification of a mutation in the extremely conserved motif of the PHY GAF domain strongly suggested that *HvPHYC* is the gene underlying the *eam5* locus. Protein modeling revealed that the amino-acid change occurred at a prominent position in the GAF domain at the end of a helix coming to the chromophore pocket, potentially affecting conformational flexibility of the protein (Figure S4). A mutation in this region might not be expected to alter the photochromic behavior of the protein. Future work could examine whether the reversion rates from Pfr to Pr are compromised in the HvPHYC F380S isoform.

Our study is an example of the efficient exploitation of the comprehensive barley mutant resources. More than 800 natural and induced barley mutants introgressed into the common genetic background Bowman await fine mapping and functional analysis of the causative genes (Druka *et al.* 2011).

HvPHYC modulates the circadian clock

The F380S mutation did not correspond to any known loss- or gain-of-function phytochrome allele in *Arabidopsis* (Nagatani 2010). However, the mutation was identical to the HvPHYC-e allele recently described in the Japanese winter barley Hayakiso 2 (Nishida *et al.* 2013). The authors of that study found that this allele accelerated flowering time under 16-hr and 20-hr LDs, but not under 12-hr SDs. However, we observed the strongest effect of *eam5* under 8-hr SDs, where flowering time of Bowman(*eam5*) and Bowman differed by >60 days. It is noteworthy that the loss-of-function *PHYC* mutants in *Arabidopsis* and rice also showed acceleration of flowering in noninductive photoperiods (Monte *et al.* 2003; Takano *et al.* 2005; Balasubramanian *et al.* 2006).

Osugi *et al.* (2011) have shown that light signals mediated by the PHYB/PHYC heterodimer in rice can induce expression of *Ghd7*, a floral repressor of *Hd3*, which is the rice ortholog of *FT*, and thus delay flowering. They also argued that phytochromes do not control the gating of *Ghd7* and therefore do not affect flowering through entrainment of the circadian clock. Likewise, the complete loss of three phytochromes in rice did not influence the expression of circadian-clock genes, while it affected the expression of *Hd3* (Izawa *et al.* 2002). Similarly, Nishida *et al.* (2013) reported that, in barley, HvPHYC F380S (HvPhyC-e) caused an upregulation of *HvFT1* under LDs, but did not change the expression of clock genes under the diurnal LD regime. Hence they suggested that HvPHYC F380S does not affect the circadian clock. Based on the expression patterns of clock genes measured under circadian LL conditions, we conclude that HvPHYC F380S markedly disturbed the circadian expression of clock genes in Bowman(*eam5*) and the Japanese cultivars carrying the F380S mutation. For example, *HvCCA1* did not oscillate under LL conditions. Changes in clock gene expression, especially the absence of *HvCCA1* oscillations in Bowman (*eam5*), are reminiscent of expression changes observed in the *eam8* and *eam10* mutants carrying mutations in *HvELF3* and *HvLUX1*, respectively (Faure *et al.* 2012; Campoli *et al.* 2013; Figure S5).

It is known that *Arabidopsis* phytochromes control the period of the circadian clock; deficiency of phytochromes causes a period lengthening, whereas overexpression of phytochromes results in a period shortening (Somers *et al.* 1998; Hu *et al.* 2013). Additionally, Hu *et al.* (2013) demonstrated that *phyABDE* and *phyABCDE Arabidopsis* mutants retained robust clock rhythms and thus argued that phytochromes are not required for clock maintenance. By contrast, we showed that a mutation in HvPHYC was linked to the disruption of circadian oscillations of barley clock genes. Our results offer new perspectives on the role of PHYC in controlling the circadian clock and downstream light signaling pathways.

As has been shown for Bowman(*eam8*) and Bowman (*eam10*) (Faure *et al.* 2012; Campoli *et al.* 2013), early flowering of Bowman(*eam5*) was associated with an upregulation of *HvFT1* under both LD and SD conditions (Figure 2). Consequently, *eam5* caused an induction of the LD photoperiod pathway under noninductive SD conditions. Interestingly, a recent study in wheat demonstrated that the loss of a functional PhyC resulted in a drastic downregulation of PPD1 and TaFT1 and late flowering under LDs and SDs (Chen *et al.* 2014). This is in line with our findings, which suggest that PhyC is important in light perception or signaling to downstream components of the photoperiod pathway.

In *Arabidopsis*, ELF3 together with ELF4 and LUX form the so-called evening complex (EC) and repress transcription

---

subjective nights, respectively. Values represent averages of two biological and two technical replicates of expression values relative to *HvActin* plus/minus standard deviation. *VRN-H1* expression in Bowman(*eam5*) and *HvFT1* expression under SDs in both genotypes were not detected. Significant differences in gene expression are indicated by asterisks (*$P < 0.05$).

of PRRs (Dixon *et al.* 2011; Herrero *et al.* 2012). The transcriptional targets of the EC genes seem conserved in barley. HvELF3 and HvLUX1 act as repressors of the barley PRR gene *Ppd-H1*, which in turn affects *HvFT1* expression and flowering time (Faure *et al.* 2012). Indeed, we observed genetic interactions between *eam5* and *Ppd-H1* as demonstrated for *eam8* and *eam10* (Figure 1). Additionally, upregulation of *Ppd-H1* in Bowman(*eam5*) suggested that *eam5*, like *eam8* and *eam10*, controlled the expression of this gene (Figure S5). In this context, it is interesting to note that variation at *eam5* had similar effects on SAM development as variation at *Ppd-H1*. Both affected primarily inflorescence development (Figure S1, Campoli *et al.* 2012b).

Similarities in the effects of *eam5*, *eam8*, and *eam10* on the expression of circadian clock genes and *HvFT1* (Figure S5) suggest that all three genes may act in the same pathway. This is in line with the findings that phytochromes modulate the function of ELF3 in *Arabidopsis*. There it is noted that PHYB interacts with the ELF3 protein and represses its activity (Liu *et al.* 2001; Kolmos *et al.* 2011). We thus speculate that HvPHYC might modulate the repressive activity of the evening complex genes. However, further mechanistic evidence is required to solidify the hypothesis that HvPHYC F380S affects accumulation and activity of the HvELF3 protein.

To investigate genetic diversity at *HvPHYC*, we resequenced in addition to Bowman and Bowman(*eam5*) a diverse set of 109 *HvPHYC* genotypes and added three *HvPHYC* alleles from the GenBank. The prevalence of two major haplotypes and the nucleotide diversity index, which was 2 to 16 times lower than reported for other barley genes (Russell *et al.* 2004; Morrell *et al.* 2005, 2013; Kilian *et al.* 2006; Xia *et al.* 2012), indicated that PhyC was conserved and presumably under selective constraints. It is tempting to speculate that reduced nucleotide diversity at *HvPHYC* could be an indirect effect of its tight linkage to *VRN-H1*, which mediates an adaptive trait such as vernalization response (Beales *et al.* 2005; Hemming *et al.* 2009). It is intriguing that the mutant PhyC380 allele was detected in 11 genotypes with a common geographic origin in Japan, suggesting that this mutant allele was targeted by breeders.

Molecular taxonomists have widely used phytochromes in phylogenetic studies (Mathews *et al.* 1995). This led to the accumulation of a large number of PHY sequences from very diverse plant and bacteria species. We used these data to infer a functional effect of the observed amino-acid substitutions based on the extent of their conservation. Remarkably, except for the two amino-acid substitutions, L364D and F380S (haplotypes 4 and 7), which we linked to the functionally distinct *HvPHYC* alleles, other substitutions were within variable motifs and thus presumably nonfunctional.

In summary, we successfully applied a mapping-by-sequencing approach to pinpoint a mutation in *HvPHYC* as a candidate underlying the *eam5* locus in barley. We demonstrated that this mutation disrupts the circadian clock and results in an acceleration of flowering under LDs and noninductive SDs. Such interaction of phytochromes and the circadian clock has not been reported before and opens new perspectives on the role of PHYC in controlling the circadian clock and downstream light signaling pathways. We demonstrate that *HvPHYC* is characterized by low levels of genetic diversity in wild and cultivated barley germplasm. Interestingly, HvPHYC F380S was selected in cultivars from Japan, and may thus provide a selective advantage in these environments.

Literature Cited

Badr, A., K. Müller, R. Schäfer-Pregl, H. El Rabey, S. Effgen *et al.*, 2000   On the origin and domestication history of barley (*Hordeum vulgare*). Mol. Biol. Evol. 17: 499–510.

Balasubramanian, S., S. Sureshkumar, M. Agrawal, T. P. Michael, C. Wessinger *et al.*, 2006   The *PHYTOCHROME C* photoreceptor gene mediates natural variation in flowering and growth responses of *Arabidopsis thaliana*. Nat. Genet. 38: 711–715.

Beales, J., D. Laurie, and K. M. Devos, 2005   Allelic variation at the linked *AP1* and *PhyC* loci in hexaploid wheat is associated but not perfectly correlated with vernalization response. Theor. Appl. Genet. 110: 1099–1107.

Butler, W., and H. C. Lane, 1965   Dark transformations of phytochromes in vivo. II. Plant Physiol. 40: 13–17.

Campoli, C., B. Drosse, B. Searle, G. Coupland, and M. von Korff, 2012a   Functional characterization of *HvCO1*, the barley (*Hordeum vulgare*) flowering time ortholog of *CONSTANS*. Plant J. 9: 868–880.

Campoli, C., M. Shtaya, S. J. Davis, and M. von Korff, 2012b   Expression conservation within the circadian clock of a monocot: natural variation at barley *Ppd-H1* affects circadian expression of flowering time genes, but not clock orthologs. BMC Plant Biol. 2: 97.

Campoli, C., A. Pankin, B. Drosse, C. M. Casao, S. J. Davis *et al.*, 2013   *HvLUX1* is a candidate gene underlying the early maturity 10 locus in barley: phylogeny, diversity, and interactions with the circadian clock and photoperiodic pathways. New Phytol. 99: 1045–1059.

Chen, A., C. Li, W. Hu, M. L. Lau, H. Lin *et al.*, 2014   PHYTOCHROME C plays a major role in the acceleration of wheat flowering under long day photoperiod. Proc. Natl. Acad. Sci. USA DOI: 10.1073/pnas.1409795111.

Childs, K., F. Miller, M. M. Cordonnier-Pratt, L. H. Pratt, P. W. Morgan *et al.*, 1997   The sorghum photoperiod sensitivity gene, *Ma3*, encodes a phytochrome B. Plant Physiol. 113: 611–619.

Choi, Y., G. Sims, S. Murphy, J. R. Miller, and A. P. Chan, 2012   Predicting the functional effect of amino acid substitutions and indels. PLoS ONE 7: e46688.

Close, T., P. Bhat, S. Lonardi, Y. Wu, N. Rostoks *et al.*, 2009   Development and implementation of high-throughput SNP genotyping in barley. BMC Genomics 10: 582.

Conesa, A., S. Götz, J. M. García-Gómez, J. Terol, M. Talón *et al.*, 2005   Blast2GO: a universal tool for annotation, visualization and analysis in functional genomics research. Bioinformatics 21: 3674–3676.

Crooks, G., G. Hon, J. M. Chandonia, and S. E. Brenner, 2004   WebLogo: a sequence logo generator. Genome Res. 14: 1188–1190.

Davis, S., 2002   Photoperiodism: the coincidental perception of the season. Curr. Biol. 12: R841–R843.

Dixon, L., K. Knox, L. Kozma-Bognar, M. M. Southern, A. Pokhilko *et al.*, 2011   Temporal repression of core circadian genes is mediated through EARLY FLOWERING 3 in Arabidopsis. Curr. Biol. 21: 120–125.

Druka, A., J. Franckowiak, U. Lundqvist, N. Bonar, J. Alexander *et al.*, 2011   Genetic dissection of barley morphology and development. Plant Physiol. 155: 617–627.

Eckert, A., J. Liechty, B. R. Tearse, B. Pande, and D. B. Neale, 2010   DnaSAM: software to perform neutrality testing for large datasets with complex null models. Mol Ecol Resour 10: 542–545.

Faure, S., A. Turner, D. Gruszka, V. Christodoulou, S. J. Davis *et al.*, 2012   Mutation at the circadian clock gene *EARLY MATURITY 8* adapts domesticated barley (*Hordeum vulgare*) to short growing seasons. Proc. Natl. Acad. Sci. USA 109: 8328–8333.

Franckowiak, J., 2002   BGS 348, Early maturity 5, Eam5. Barley Genet. Newsl. 32: 109.

Franklin, K., and P. H. Quail, 2010   Phytochrome functions in Arabidopsis development. J. Exp. Bot. 61: 11–24.

Galvão, V., K. Nordström, C. Lanz, P. Sulz, J. Mathieu *et al.*, 2012   Synteny-based mapping-by-sequencing enabled by targeted enrichment. Plant J. 71: 517–526.

Habte, E., L. Müller, M. Shtaya, S. J. Davis, and M. von Korff, 2014   Osmotic stress at the barley root affects expression of circadian clock genes in the shoot. Plant Cell Environ. 36(6): 1321–1337.

Hanumappa, M., L. Pratt, M. M. Cordonnier-Pratt, and G. F. Deitzer, 1999   A photoperiod-insensitive barley line contains a light-labile Phytochrome B. Plant Physiol. 119: 1033–1040.

Hemming, M., S. Fieg, W. J. Peacock, E. S. Dennis, and B. Trevaskis, 2009   Regions associated with repression of the barley (*Hordeum vulgare*) *VERNALIZATION1* gene are not required for cold induction. Mol. Genet. Genomics 282: 107–117.

Hemming, M., W. Peacock, E. S. Dennis, and B. Trevaskis, 2008   Low-temperature and daylength cues are integrated to regulate *FLOWERING LOCUS T* in barley. Plant Physiol. 147: 355–366.

Herrero, E., E. Kolmos, N. Bujdoso, Y. Yuan, M. Wang *et al.*, 2012   EARLY FLOWERING4 recruitment of EARLY FLOWERING3 in the nucleus sustains the Arabidopsis circadian clock. Plant Cell 24: 428–443.

Hu, W., K. Franklin, R. A. Sharrock, M. A. Jones, S. L. Harmer *et al.*, 2013   Unanticipated regulatory roles for Arabidopsis phytochromes revealed by null mutant analysis. Proc. Natl. Acad. Sci. USA 110: 1542–1547.

Huang, W., P. Pérez-García, A. Pokhilko, A. J. Millar, I. Antoshechkin *et al.*, 2012   Mapping the core of the Arabidopsis circadian clock defines the network structure of the oscillator. Science 336: 75–79.

Hübner, S., M. Höffken, E. Oren, G. Haseneyer, N. Stein *et al.*, 2009   Strong correlation of the population structure of wild barley (*Hordeum spontaneum*) across Israel with temperature and precipitation variation. Mol. Ecol. 18: 1523–1536.

International Barley Sequencing Consortium (IBSC), 2012   A physical, genetic and functional sequence assembly of the barley genome. Nature 491: 711–716.

Izawa, T., T. Oikawa, N. Sugiyama, T. Tanisaka, M. Yano *et al.*, 2002   Phytochrome mediates the external light signal to repress *FT* orthologs in photoperiodic flowering of rice. Genes Dev. 16: 2006–2020.

Jain, K. B. L., 1961   Genetic studies in barley. III. Linkage relations of some plant characters. Indian J. Genet. Plant Breed. 21: 23–33.

James, G. V., V. Patel, K. J. V. Nordström, J. R. Klasen, P. A. Salomé *et al.*, 2013   User guide for mapping-by-sequencing in Arabidopsis. Genome Biol. 14: R61.

Jones, H., F. Leigh, I. Mackay, M. A. Bower, L. M. J. Smith *et al.*, 2008   Population-based resequencing reveals that the flowering time adaptation of cultivated barley originated east of the Fertile Crescent. Mol. Biol. Evol. 25: 2211–2219.

Katoh, K., and H. Toh, 2008   Recent developments in the MAFFT multiple sequence alignment program. Brief. Bioinform. 9: 286–298.

Kilian, B., H. Ozkan, J. Kohl, A. von Haeseler, F. Barale *et al.*, 2006   Haplotype structure at seven barley genes: relevance to gene pool bottlenecks, phylogeny of ear type and site of barley domestication. Mol. Genet. Genomics 276: 230–241.

Koboldt, D., K. Chen, T. Wylie, D. E. Larson, M. D. McLellan *et al.*, 2009   VarScan: variant detection in massively parallel sequencing of individual and pooled samples. Bioinformatics 25: 2283–2285.

Kolmos, E., M. Nowak, M. Werner, K. Fischer, G. Schwarz *et al.*, 2009   Integrating ELF4 into the circadian system through combined structural and functional studies. HFSP J 3: 350–366.

Kolmos, E., E. Herrero, N. Bujdoso, A. J. Millar, R. Tóth *et al.*, 2011   A reduced-function allele reveals that EARLY FLOWERING3 repressive action on the circadian clock is modulated by phytochrome signals in Arabidopsis. Plant Cell 23: 3230–3246.

Li, H., and R. Durbin, 2009   Fast and accurate short read alignment with Burrows-Wheeler transform. Bioinformatics 25: 1754–1760.

Li, H., B. Handsaker, A. Wysoker, T. Fennell, J. Ruan *et al.*, 2009   The Sequence Alignment/Map format and SAMtools. Bioinformatics 25: 2078–2079.

Liu, X., M. Covington, C. Fankhauser, J. Chory, and D. R. Wagner, 2001   *ELF3* encodes a circadian clock-regulated nuclear protein that functions in an Arabidopsis PHYB signal transduction pathway. Plant Cell 13: 1293–1304.

Loytynoja, A., and N. Goldman, 2005   An algorithm for progressive multiple alignment of sequences with insertions. Proc. Natl. Acad. Sci. USA 102: 10557–10562.

Mascher, M., G. Muehlbauer, D. S. Rokhsar, J. Chapman, J. Schmutz *et al.*, 2013a   Anchoring and ordering NGS contig assemblies by population sequencing (POPSEQ). Plant J. 76: 718–727.

Mascher, M., T. Richmond, D. J. Gerhardt, A. Himmelbach, L. Clissold *et al.*, 2013b   Barley whole exome capture: a tool for genomic research in the genus *Hordeum* and beyond. Plant J. 76: 494–505.

Mathews, S., 2010   Evolutionary studies illuminate the structural-functional model of plant phytochromes. Plant Cell 22: 4–16.

Mathews, S., M. Lavin, and R. A. Sharrock, 1995   Evolution of the phytochrome gene family and its utility for phylogenetic analyses of angiosperms. Ann. Mo. Bot. Gard. 82: 296–321.

Monte, E., J. Alonso, J. R. Ecker, Y. Zhang, X. Li *et al.*, 2003   Isolation and characterization of phyC mutants in Arabidopsis reveals complex crosstalk between phytochrome signaling pathways. Plant Cell 15: 1962–1980.

Morrell, P., A. Gonzales, K. K. Meyer, and M. T. Clegg, 2013   Resequencing data indicate a modest effect of domestication on diversity in barley: a cultigen with multiple origins. J. Hered. 105: 253–264.

Morrell, P., D. Toleno, K. E. Lundy, and M. T. Clegg, 2005   Low levels of linkage disequilibrium in wild barley (*Hordeum vulgare*

ssp. *spontaneum*) despite high rates of self-fertilization. Proc. Natl. Acad. Sci. USA 102: 2442–2447.

Nagatani, A., 2010 Phytochrome: structural basis for its functions. Curr. Opin. Plant Biol. 13: 565–570.

Nishida, H., D. Ishihara, M. Ishii, T. Kaneko, H. Kawahigashi *et al.*, 2013 Phytochrome C is a key factor controlling long-day flowering in barley. Plant Physiol. 163: 804–814.

Onai, K., and M. Ishiura, 2005 *PHYTOCLOCK 1* encoding a novel GARP protein essential for the Arabidopsis circadian clock. Genes Cells 10: 963–972.

Osugi, A., H. Itoh, K. Ikeda-Kawakatsu, M. Takano, and T. Izawa, 2011 Molecular dissection of the roles of phytochrome in photoperiodic flowering in rice. Plant Physiol. 157: 1128–1137.

Pettersen, E., T. Goddard, C. C. Huang, G. S. Couch, D. M. Greenblatt *et al.*, 2004 UCSF Chimera–a visualization system for exploratory research and analysis. J. Comput. Chem. 25: 1605–1612.

Pokhilko, A., A. Fernández, K. D. Edwards, M. M. Southern, K. J. Halliday *et al.*, 2012 The clock gene circuit in Arabidopsis includes a repressilator with additional feedback loops. Mol. Syst. Biol. 8: 574.

Quevillon, E., V. Silventoinen, S. Pillai, N. Harte, N. Mulder *et al.*, 2005 InterProScan: protein domains identifier. Nucleic Acids Res. 33: W116–W120.

Rollins, J. A., B. Drosse, M. A. Mulki, S. Grando, M. Baum *et al.*, 2013 Variation at the vernalisation genes *Vrn-H1* and *Vrn-H2* determines growth and yield stability in barley (*Hordeum vulgare*) grown under dryland conditions in Syria. Theor. Appl. Genet. 126(11): 2803–2824.

Russell, J., A. Booth, J. Fuller, B. Harrower, P. Hedley *et al.*, 2004 A comparison of sequence-based polymorphism and haplotype content in transcribed and anonymous regions of the barley genome. Genome 47: 389–398.

Saïdou, A., C. Mariac, V. Luong, J. L. Pham, G. Bezançon *et al.*, 2009 Association studies identify natural variation at *PHYC* linked to flowering time and morphological variation in pearl millet. Genetics 182: 899–910.

SAS Institute, 2009 *The SAS system for Windows, release 9.1.3*, SAS Institute, Cary, NC.

Schneeberger, K., S. Ossowski, C. Lanz, T. Juul, A. H. Petersen *et al.*, 2009 SHOREmap: simultaneous mapping and mutation identification by deep sequencing. Nat. Methods 6: 550–551.

Schöning, J., and D. Staiger, 2005 At the pulse of time: protein interactions determine the pace of circadian clocks. FEBS Lett. 579: 3246–3252.

Simpson, J., K. Wong, S. D. Jackman, J. E. Schein, S. J. Jones *et al.*, 2009 ABySS: a parallel assembler for short read sequence data. Genome Res. 19: 1117–1123.

Somers, D., P. Devlin, and S. A. Kay, 1998 Phytochromes and cryptochromes in the entrainment of the Arabidopsis circadian clock. Science 282: 1488–1490.

Szücs, P., I. Karsai, J. von Zitzewitz, K. Mészáros, L. L. D. Cooper *et al.*, 2006 Positional relationships between photoperiod response QTL and photoreceptor and vernalization genes in barley. Theor. Appl. Genet. 112: 1277–1285.

Takano, M., N. Inagaki, X. Xie, N. Yuzurihara, F. Hihara *et al.*, 2005 Distinct and cooperative functions of phytochromes A, B, and C in the control of deetiolation and flowering in rice. Plant Cell 17: 3311–3325.

Turner, A., J. Beales, S. Faure, R. P. Dunford, and D. A. Laurie, 2005 The pseudo-response regulator *Ppd-H1* provides adaptation to photoperiod in barley. Science 310: 1031–1034.

von Korff, M., J. Léon, and K. Pillen, 2010 Detection of epistatic interactions between exotic alleles introgressed from wild barley (*H. vulgare* ssp. *spontaneum*). Theor. Appl. Genet. 121: 1455–1464.

von Korff, M., H. Wang, J. Leon, and K. Pillen, 2006 AB-QTL analysis in spring barley: II. Detection of favourable exotic alleles for agronomic traits introgressed from wild barley (*H. vulgare* ssp. *spontaneum*). Theor. Appl. Genet. 112: 1221–1231.

Waddington, S., P. Cartwright, and P. C. Wall, 1983 A quantitative scale of spike initial and pistil development in barley and wheat. Ann. Bot. (Lond.) 51: 119–130.

Wang, G., I. Schmalenbach, M. von Korff, J. Léon, B. Kilian *et al.*, 2010 Association of barley photoperiod and vernalization genes with QTLs for flowering time and agronomic traits in a DH-population and a set of wild barley introgression lines. Theor. Appl. Genet. 120: 1559–1574.

Xia, Y., Z. Ning, G. Bai, R. Li, G. Yan *et al.*, 2012 Allelic variations of a light harvesting chlorophyll a/b-binding protein gene (*Lhcb1*) associated with agronomic traits in barley. PLoS ONE 7: e37573.

Yan, L., A. Loukoianov, G. Tranquilli, M. Helguera, T. Fahima *et al.*, 2003 Positional cloning of the wheat vernalization gene *VRN1*. Proc. Natl. Acad. Sci. USA 100: 6263–6268.

Yan, L., A. Loukoianov, A. Blechl, G. Tranquilli, W. Ramakrishna *et al.*, 2004 The wheat *VRN2* gene is a flowering repressor down-regulated by vernalization. Science 303: 1640–1644.

Zakhrabekova, S., S. Gough, I. Braumann, A. H. Müller, J. Lundqvist *et al.*, 2012 Induced mutations in circadian clock regulator *Mat-a* facilitated short-season adaptation and range extension in cultivated barley. Proc. Natl. Acad. Sci. USA 109: 4326–4331.

Zhang, Y., 2008 I-TASSER server for protein 3D structure prediction. BMC Bioinformatics 9: 40.

Communicating editor: J. Borevitz

GENETICS

Mapping-by-Sequencing Identifies *HvPHYTOCHROME C* as a Candidate Gene for the *early maturity 5* Locus Modulating the Circadian Clock and Photoperiodic Flowering in Barley

Artem Pankin, Chiara Campoli, Xue Dong, Benjamin Kilian, Rajiv Sharma, Axel Himmelbach, Reena Saini, Seth J Davis, Nils Stein, Korbinian Schneeberger, and Maria von Korff
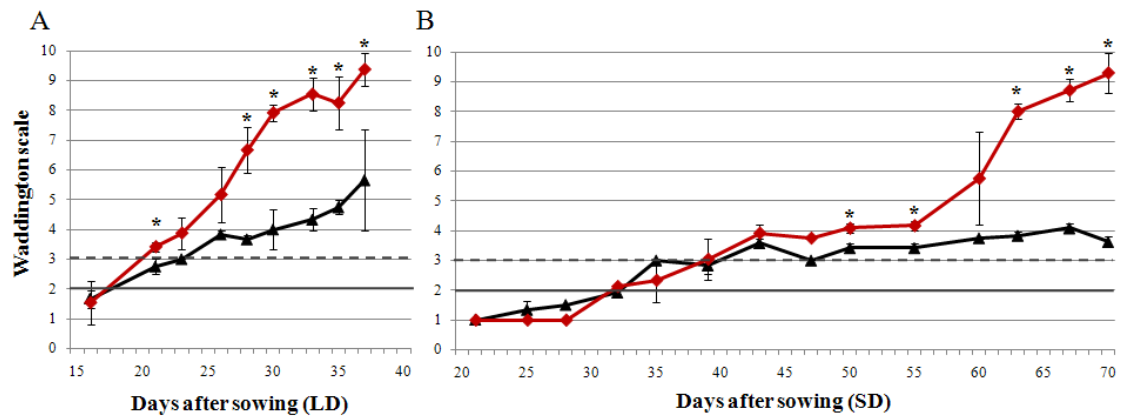
Figure S1 Meristem development in wild type Bowman and Bowman(*eam10)* mutant plants. Apex development assessed by the Waddington scale (WS) under (A) long- (LD; 16 h) and (B) short- (SD; 8 h) day conditions in Bowman (black lines) and Bowman(*eam5*) (red lines). Double ridge formation (WS2) and the initiation of internode elongation (WS3) are indicated by full and dashed lines, respectively. Values are means of three plants plus/minus standard deviation. Significant differences in meristem development are indicated by asterisks (*P < 0.05).

A. Pankin *et al.*
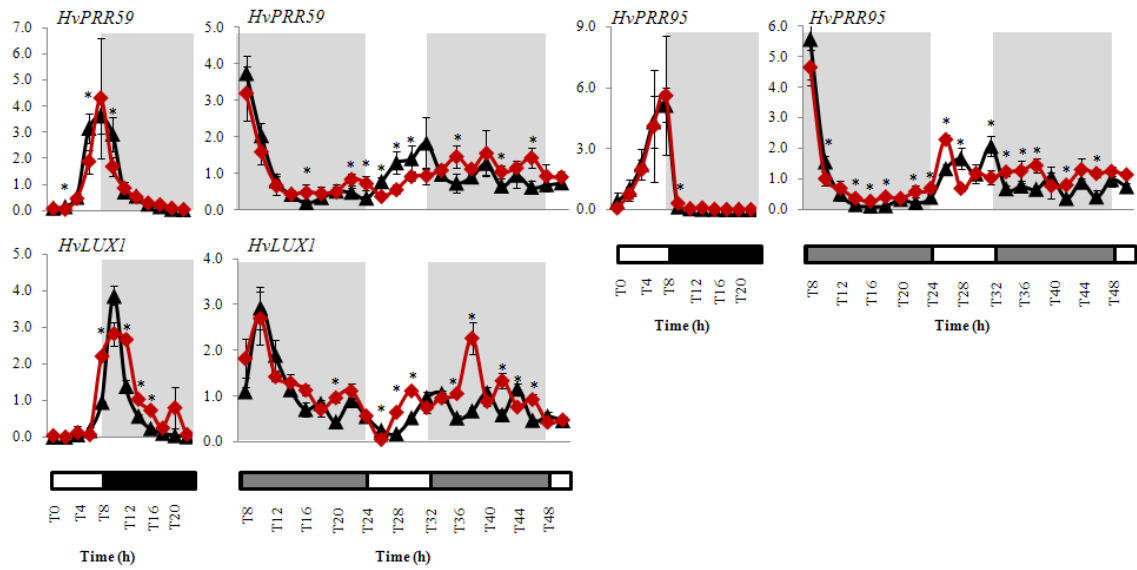
Figure S2 Expression patterns of circadian clock genes. Expression of *HvPRR59, HvPRR95* and *HvLUX1* in Bowman (black lines) and Bowman(*eam5)* plants (red lines) under short-day and continuous-light conditions. White, black and grey bars indicate days, nights and subjective nights, respectively. Expression values represent averages of two biological and two technical replicates relative to *HvActin* plus/minus standard deviation. Significant differences in gene expression are indicated by asterisks (*P < 0.05).
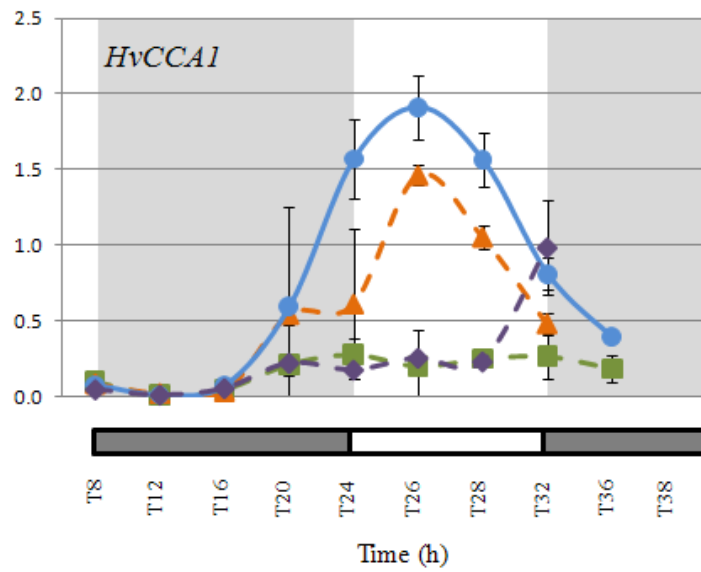
Figure S3 Expression levels of *HvCCA1* in WT and mutant HvPHYC F380S lines. Expression of *HvCCA1* in Azumamugi (orange), Hayachinemugi (green) and its parental lines Kaikei 84 (purple) and Yukiwarimugi (blue). Full and dashed lines indicate genotypes with a wild type or a mutated *HvPHYC* allele, respectively. Plants were grown under short days for two weeks, and then released into continuous light. Samples were taken every 4 hours starting from the beginning of the first subjective night (T8). White and grey bars indicate days and subjective nights, respectively. Expression values are averages of two biological and two technical replicates relative to *HvActin* plus/minus standard deviation.
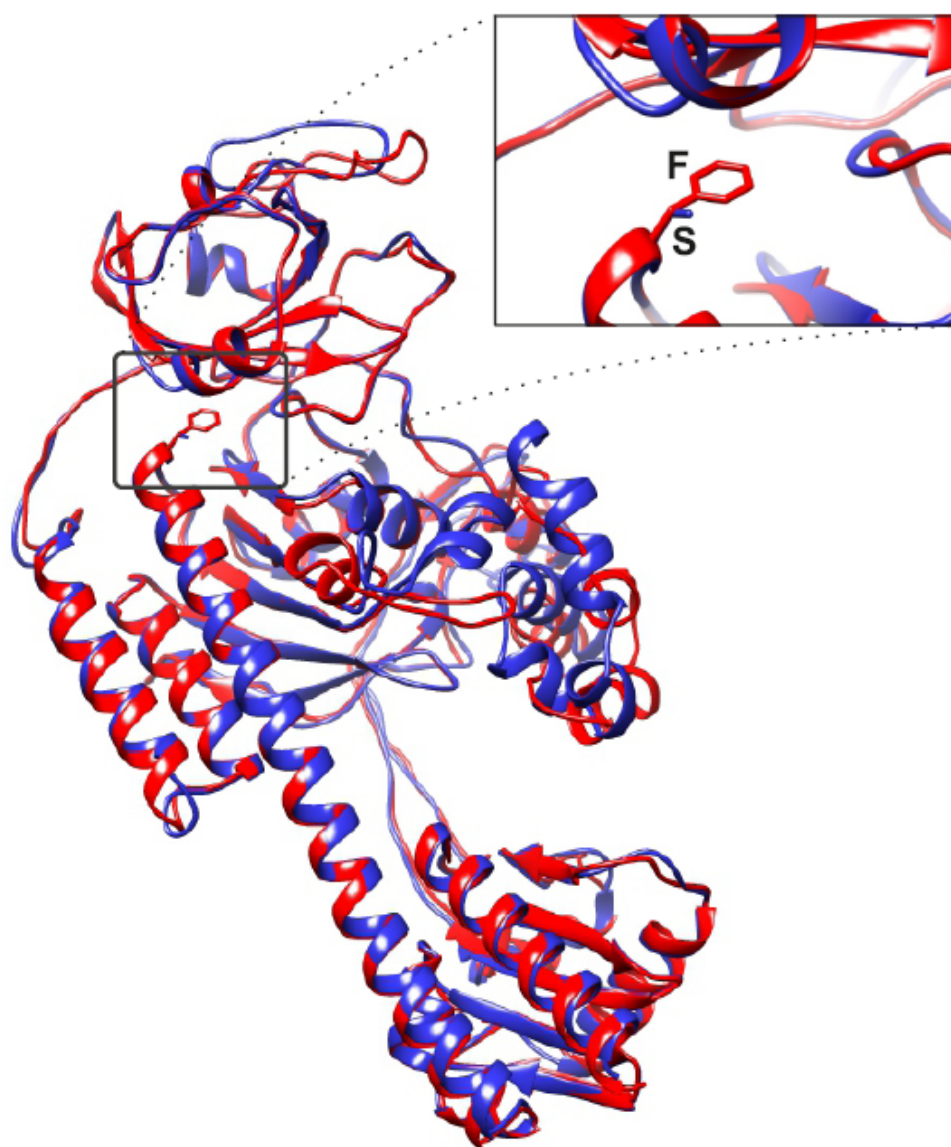
Figure S4 Structural model from I-TASSER of barley HvPHYC. In red is the wild type model and this is overlaid in blue with the eam5-derived variant (HvPHYC F380S). The amino-acid change is at the end of an alpha helix and outside of the chromophore binding pocket.
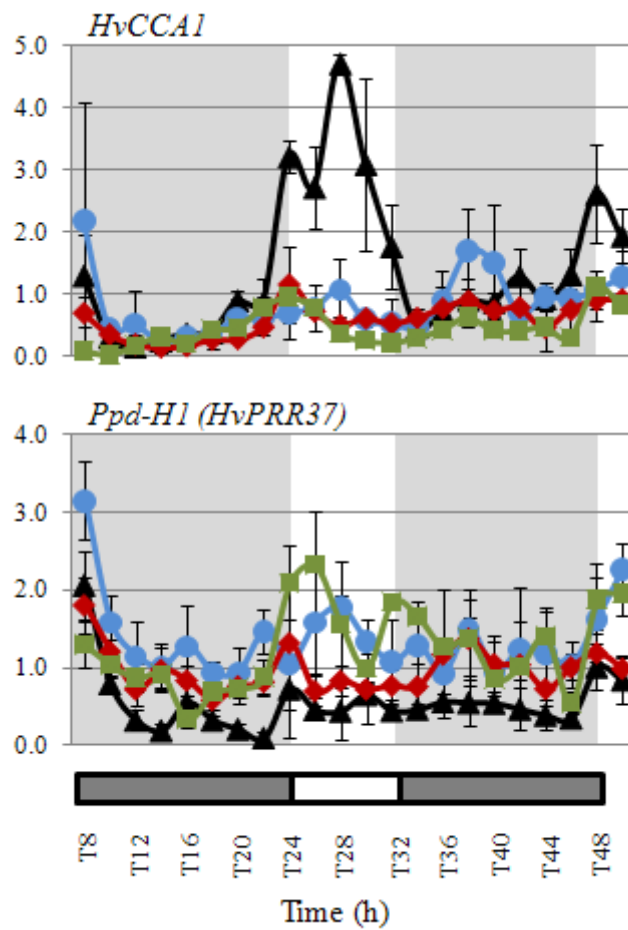
Figure S5 Expression profiles of the clock genes in *eam5* and previously described clock mutants. Expression of *HvCCA1* and *Ppd-H1 (HvPRR37)* in Bowman (black lines), Bowman(*eam5)* (red lines), Bowman(*eam10)* (blue lines; Campoli et al., 2013) and Bowman (*eam8*) (green lines; Faure et al., 2012). Plants were grown under short days for two weeks, and then released in continuous light. Samples were taken every 2 hours starting from the beginning of the first subjective night (T8). White and grey bars indicate days and subjective nights, respectively. Values represent average of two biological and two technical replicates of expression values relative to *HvActin* plus/minus standard deviation.

A. Pankin *et al.*
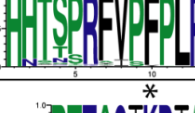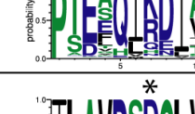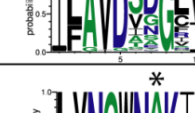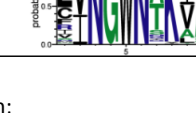
Table S1 Fifteen polymorphic haplotypes of *HvPHYC*.

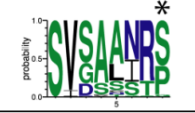| Haplotype	Position (bp) relative to the start codon of the reference Morex *HvPHYC* gene (DQ238106)																					No. of samples
	149	175	206	209	210	249	415	906	920	1008	1027	1091	1139	1239	1403	1491	1659	1722	1764	1921	1945	
1	-	-	-	-	-	-	-	-	-	-	-	-	-	-	-	-	-	-	-	-	-	70
2	-	-	-	-	-	-	-	-	-	-	-	-	-	-	-	T	-	-	-	-	-	14
3	-	-	-	-	-	-	-	A	-	-	-	-	-	-	-	-	-	T	-	-	-	4
4	-	-	-	-	-	-	-	-	-	-	-	-	C	-	-	-	-	-	-	-	-	11
5	-	-	-	-	-	-	A	-	-	-	-	-	-	-	-	-	-	-	-	-	A	2
6	-	-	-	-	-	-	-	-	-	-	-	-	-	-	G	-	-	-	-	-	-	2
7	-	-	-	-	-	-	-	-	-	-	C	C	-	-	-	-	-	-	-	-	-	1
8	-	-	-	-	-	-	-	-	-	-	-	-	-	-	-	-	-	-	G	-	-	1
9	-	-	-	A	C	-	-	-	-	-	-	A	-	-	-	-	-	-	-	-	A	1
10	-	-	T	-	-	-	-	-	-	-	-	-	-	-	-	-	-	-	-	-	-	1
11	-	-	-	-	-	T	-	-	T	A	-	-	-	-	T	-	-	-	-	A	A	1
12	-	-	-	-	-	-	-	-	-	-	-	-	-	-	-	T	A	-	-	-	-	1
13	A	-	-	-	-	-	-	-	-	-	-	-	-	-	-	-	-	-	-	-	-	3
14	-	A	-	-	-	-	-	-	-	-	-	-	-	-	-	-	-	-	-	-	-	1
15	-	-	-	-	-	-	-	T	-	-	-	-	-	-	-	T	-	-	-	-	-	1

n = 114

Non-synonymous single nucleotide polymorphisms (nsSNP) are highlighted in red. Position of the nsSNP found in *HvPHYC* from Bowman(*eam5*) is underlined.

Table S2 Non-synonymous SNPs in the exon 1 of *HvPHYC* and conservation of the corresponding amino-acid (a.a.) residues.

SNP ID[1]	A.a. substitution[2]	# of sequences in the logo	Motif logo[3]
149	S50Y	72	
175	S59T	231	
209-210	Y70F	249	
415	V139I	966	
920	S307L	4298	
1027	I343V	4331	
1091	L364D	4340	
1139	F380S	4353	
1403	K468R	4107	
1921	V641I	1610	
1945	G649S	1610	

1 - SNP positions given from the first nucleotide of the *HvPHYC* start codon;

2 - Deleterious a.a. substitutions as predicted by PROVEAN (cut-off score -2,5) are highlighted in red;

3 - substituted a.a. residues marked within the motifs with asterisks; letters in black, green and blue refer to hydrophobic, neutral and hydrophilic a.a. residues, respectively.

Table S3 Accessions used for the *HvPHYC* re-sequencing and haplotype analysis.

Hordeum species	Genotype*	Status	Growth habit	Origin	*HvPHYC* haplotype
vulgare subsp. *vulgare*	Arta	cultivar	winter	Syria	1
	Asahi 5	cultivar	n.d.**	Japan	4
	Azumamugi	cultivar	n.d.	Japan	7
	B.E. 22 (ASA)	cultivar	n.d.	Pakistan	2
	B1K-70-01	cultivar	spring	Israel	1
	B1K-70-02	cultivar	spring	Israel	1
	Bowman	cultivar	n.d.	USA	14
	Bowman(*eam5*)	introgression line	spring	n.d.	4
	Dicktoo	cultivar	n.d.	USA	15
	Erectoides 16	cultivar	n.d.	Sweden	1
	G-391 F	cultivar	spring	Italy	2
	G-413 I	cultivar	n.d.	Czech Republic	1
	Ghara 1 (1609)	cultivar	n.d.	Nepal	3
	Hamidiye 85	cultivar	spring	Turkey	1
	Haruna Nijo	cultivar	spring	Japan	4
	Hayachinemugi	cultivar	n.d.	Japan	4
	Hayakiso 2	cultivar	winter	Japan	4
	Hayakiso 3	cultivar	n.d.	Japan	1
	Indian dwarf	cultivar	n.d.	n.d.	1
	Indo Omugi	cultivar	spring	Taiwan	1
	Ishuku Shirazu	cultivar	spring	Japan	4
	Kagoshima Gold	cultivar	n.d.	Japan	1
	Kaikei 84	cultivar	n.d.	Japan	4
	Kanto Nijo 3	cultivar	n.d.	Japan	4
	Kawasaigoku	cultivar	spring	Japan	4
	Keel	cultivar	spring	Australia	1
	Kinai 5	cultivar	n.d.	Japan	1
	Kindoku	cultivar	n.d.	Sweden	1
	Kompolti	cultivar	n.d.	Hungary	2
	L871	cultivar	spring	Egypt	1
	Mari	cultivar	n.d.	Sweden	1
	Marthe	cultivar	spring	Germany	1
	Morex	cultivar	spring	USA	1
	Mota 4 (1-24-13)	cultivar	n.d.	Ethiopia	1
	Mota 6 (1-24-15)	cultivar	n.d.	Ethiopia	1
	Omugi 15	cultivar	n.d.	Japan	4

Rum	cultivar	n.d.	Jordand	1
Saikai Kawa 24	cultivar	n.d.	Japan	4
Shiga Hayakiso 1	cultivar	n.d.	Japan	1
Sladoran	cultivar	winter	Turkey	2
Tadmor	cultivar	winter	Syria	1
Tainan 2	cultivar	n.d.	Taiwan	1
Turkey 759	cultivar	n.d.	Turkey	1
Yarmouk	cultivar	n.d.	Lebanon	2
Yercil 147	cultivar	winter	Turkey	2
Zairai 1	cultivar	n.d.	Taiwan	1
Zairai 2	cultivar	n.d.	Taiwan	1
B1K-55-01	landrace	n.d.	Israel	2
B1K-55-02	landrace	n.d.	Israel	1
B1K-55-06	landrace	spring	Israel	2
G-1573 A	landrace	n.d.	Syria	1
G-398 H	landrace	n.d.	Ethiopia	2
G-400 H	landrace	n.d.	Egypt	1
G-404 H	landrace	spring	Tibet	3
G-423 H	landrace	n.d.	Ethiopia	1
G-434 H	landrace	n.d.	Ethiopia	1
G-439 H	landrace	spring	Yemen	1
G-440 E	landrace	n.d.	n.d.	1
LR 1887	landrace	n.d.	n.d.	1
vulgare subsp. *spontaneum*	B1K-02-18	wild	n.d.	Israel	9
	B1K-03-07	wild	n.d.	Israel	1
	B1K-05-13	wild	n.d.	Israel	5
	B1K-08-13	wild	n.d.	Israel	5
	B1K-08-18	wild	n.d.	Israel	10
	B1K-13-01	wild	n.d.	Israel	2
	B1K-17-13	wild	n.d.	Israel	1
	B1K-21-02	wild	n.d.	Israel	1
	B1K-22-06	wild	n.d.	Israel	1
	B1K-22-10	wild	n.d.	Israel	1
	B1K-33-13	wild	n.d.	Israel	1
	HID-1	wild	winter	Iraq	1
	HID-10	wild	n.d.	Iraq	1
	HID-101	wild	winter	Syria	1
	HID-104	wild	n.d.	Syria	13
	HID-107	wild	winter	Jordan	2
	HID-109	wild	winter	Syria	12
	HID-114	wild	n.d.	Lebanon	1

	HID-122	wild	n.d.	Jordan	11
	HID-136	wild	winter	Iran	1
	HID-137	wild	n.d.	Turkey	13
	HID-140	wild	winter	Iraq	13
	HID-145	wild	n.d.	Israel	2
	HID-2	wild	n.d.	Iraq	1
	HID-24	wild	n.d.	Iran	3
	HID-257	wild	n.d.	Israel	1
	HID-301	wild	n.d.	Iran	1
	HID-309	wild	n.d.	Iran	2
	HID-330-1	wild	n.d.	n.d.	1
	HID-366	wild	n.d.	Iran	1
	HID-377-1	wild	n.d.	Israel	1
	HID-377-2	wild	n.d.	Israel	1
	HID-44	wild	n.d.	Iran	1
	HID-46	wild	n.d.	Iran	1
	HID-54	wild	n.d.	Turkey	2
	HID-55	wild	n.d.	Turkey	1
	HID-56	wild	n.d.	Turkey	1
	HID-70	wild	n.d.	Turkey	1
	HID-85	wild	n.d.	Turkey	1
	HID-96	wild	n.d.	Jordan	1
	HID-99	wild	winter	Syria	1
	HP-02-3	wild	n.d.	Turkey	1
	HP-03-2	wild	n.d.	Turkey	1
	HP-10-4	wild	n.d.	Turkey	1
	HP-10-5	wild	n.d.	Turkey	1
	HP-11-1	wild	n.d.	Turkey	1
	HP-13-2	wild	n.d.	Turkey	8
	HP-15-3	wild	winter	Turkey	6
	HP-15-5	wild	winter	Turkey	6
	HP-24-1	wild	winter	Turkey	1
	HP-26-1	wild	winter	Turkey	1
	HP-27-2	wild	winter	Turkey	1
agriocrithon	B1K-52-01	wild	n.d.	Israel	1
	HID-383-1	wild	winter	China	3
	HID-383-3	wild	n.d.	China	1

* - genotypes carrying the wild-type *HvVRN1* allele are highlighted in bold; allelic composition at *HvVRN-H1* in other genotypes is unknown; ** - n.d., no data.

Table S4 SCAR and CAPS markers for genotyping, sequencing and real-time experiments: PCR primers and amplification regimes.

	Primer	Sequence (5'-3')	Fragment size (bp)[*]	Ta[**]	Cycle[***]	Restric-tion enzyme	Digested fragment size[*]
Allele-specific SCAR and CAPS markers	PIFcaps_f	GAGCAGTACGCGCACTTC	301	58	A	*Hga*I	30+270/30+80+190
	PIFcaps_r	CTTTTGTTTGGGTGTATCGC					
	PHYCcaps_f	GGTCCTAATGCAAGGCATGT	880	62	A	*Btg*I	650+230/ 650+160+70
	PHYCcaps_r	CTCTTGCTGTTGAGCTGTGC					
	CK2Acaps_f	GTTTGTCTGCGCATGCGTG	410	60	B	*Acu*I	300+110/410
	CK2Acaps_r	ATGTTGGACAGAACATTCACAC					
	VIP4.1f	TGCTGGGATGTTATCCATG	200/350	57	B	none	
	VIP4.1r	GTGAATTGTAACAGCTCGC					
	VIP4.2f	CATGGGTGTTGGAATAATTG	180/200	57	B	none	
	VIP4.2r	ACCAAATGTCATTACGATCTC					
	VRN-H1f	AATACGACTCACTATAGGGGAAAACTTGAACAAC ACCAGAACC	320/360	50	C	none	
	VRN-H1r	TTCTGCATAAGAGTAGCGCTCAT					
VIP4 sequencing	seqVIP4.1f	ATGCAACTACTGATTGGCG	450	61	A	none	
	seqVIP4.1r	CTCAATCTCTTCGTTTGG					
	seqVIP4.2f	ATGCATCCAACAAGTCCC	900	63	A	none	
	seqVIP4.2r	ACTCACTCGATCAGGTTG					
HvPHYC exon 1 sequencing	Ex1seq_1f	CCCGTCCTTCTCCACAAAAG	1100	62	A	none	
	Ex1seq_1r	GAGCCACAGAGGCTGATAGG					
	Ex1seq_2f	ACTACCCGGCAACTGACATC	1200	62	A	none	
	Ex1seq_2r	ACAGAATCACCCTCCACGAG					
qRT-PCR primers	ELF3_DL3060F3	TGCTGTCCAAGTGTTTGAGC	242	60	D	none	
	ELF3_DL4483R3	CCTGGTTTCCTTCGGTGTTA					
	ELF4_280F	AAGAACCGGATTCTGATCCA	140	60	D	none	
	ELF4_419R	CAGGAGAGGGCGTTGTAGAG					
	PHYC_0986F	ACTACCCGGCAACTGACATC	142	60	D	none	
	PHYC_1127R	GAGCCACAGAGGCTGATAGG					

[*] Expected allele size is given in the following format: Bowman / Bowman(*eam5*).

[**] **(A)** – 98°C for 2 m; 4 touchdown cycles of 98°C – 30 s, (Ta+4) – 30 s (-1°C/cycle), 72°C – 1 m; 31 cycles of 98°C – 30 s, Ta – 30 s, 72°C – 1 m; final extension 72°C – 10 m; **(B)** – 94°C for 2 m; 4 touchdown cycles of 94°C – 30 s, (Ta+4) – 30 s (-1°C/cycle), 72°C – 30 s; 31 cycles of 94°C – 30 s, Ta – 30 s, 72°C – 30 s; final extension 72°C – 10 m; **(C)** – 94°C for 2 m; 9 touchdown cycles of 94°C – 30 s, (Ta+9) – 30 s (-1°C/cycle), 72°C – 30 s; 30 cycles of 94°C – 30 s, Ta – 30 s, 72°C – 30 s; **(D)** – 95°C for 5 m; 45 cycles of 95°C – 10 s, Ta – 10 s, 72°C – 10 s, 82°C – 10 s.

A. Pankin *et al.*